

Aus dem Centrum für Schlaganfallforschung
der Medizinischen Fakultät Charité – Universitätsmedizin Berlin

DISSERTATION

The Role of Na⁺/K⁺-ATPase Alpha Isoforms in
Spreading Depolarization

zur Erlangung des akademischen Grades
Doctor of Philosophy (PhD)

vorgelegt der Medizinischen Fakultät
Charité – Universitätsmedizin Berlin

von

Clemens Reiffurth
aus Berlin

Datum der Promotion: 18.09.2020

1. Table of contents

1. Table of contents	2
2. Abstract.....	3
3. Abstract (German)	4
4. Synopsis	6
4.1 Introduction	6
4.2 Methods	10
4.3 Results	15
4.4 Discussion	18
4.5 List of Abbreviations.....	21
4.6 Bibliography	22
5. Eidesstattliche Versicherung.....	27
6. Ausführliche Anteilserklärung	28
7. Excerpt from the Journal Summary List.....	29
8. Print copy of publication	30
9. Curriculum vitae	48
10. Complete list of publications	50
10.1 Articles.....	50
10.2 Book chapters.....	51
11. Acknowledgements.....	53

2. Abstract

The Na⁺/K⁺-ATPase is the single greatest energy consumer of brain cells and accounts for at least 50% of ATP consumption under resting conditions. When Na⁺/K⁺-ATPase function is compromised, a neuropathophysiological phenomenon is triggered, known as spreading depolarization (SD). SD is characterized by massive, unparalleled redistribution of ions across cell membranes and widespread, sustained depolarization that propagates as a wave through the gray matter of the central nervous system. SD has been shown to occur abundantly in humans in acute, life threatening medical conditions and it is widely accepted as the cellular mechanism underlying migraine aura. Mutations in ATP1A2, the gene that encodes the α 2 isoform of the Na⁺/K⁺-ATPase are associated with the occurrence of a severe subtype of migraine with aura: familial hemiplegic migraine type 2 (FHM2). This association suggests a role of the α 2 isoform in SD. Despite research on FHM2 knock-in mouse models, the roles in SD of the other two α isoforms that are expressed in the mammalian brain are largely unknown. In my thesis I investigated the role of all three brain-expressed α isoforms employing three distinct knock-out mouse lines. Combining genetic isoform ablation of Na⁺/K⁺-ATPase α 1 (ubiquitous), α 2 (astrocytic) and α 3 (neuronal) with pharmacological inhibition we compared the resulting SD phenotypes under similar conditions in the acute brain slice preparation and in vivo. We found that only α 2-deficient mice displayed increased SD susceptibility in acute brain slices. Intriguingly, this susceptibility effect was dependent on high baseline [K⁺]_o in the bathing medium and was abolished under normal [K⁺]_o in brain slices and in vivo. Furthermore, we found that the extracellular K⁺ clearance upon intense neuronal stimulation was surprisingly well compensated in α 2 deficient mice. In vivo, we found indications that the Na⁺/K⁺-ATPase α 2 isoform is implicated in modulation of the vascular tone which was evidenced by a pronounced post-SD hypoemic response that was not reproduced in α 1- or α 3-deficient mice. By contrast, deficiency of α 3 resulted in increased resistance against electrically-induced SD in vivo whereas α 1 deficiency did not affect the SD phenotype. These data support a pivotal role of the α 2 isoform in SD that is not replicated by α 1 or α 3 and that suggests specialized function through functional coupling to secondary active transporters. The observed vascular effect is particularly important in the context of migraine and stroke and warrants further research to unravel its mechanistic basis.

3. Abstract (German)

Mehr als 50% des ATP-Bedarfs unter Normalbedingungen sind auf die Na⁺/K⁺-ATPase zurückzuführen und machen diese damit zum größten Einzel-Energieverbraucher von Zellen im Gehirn. Bei Beeinträchtigung der normalen Na⁺/K⁺-ATPase-Funktion kann es im Gehirn zur Ausbildung von sog. Spreading Depolarizations (SD) kommen. Diese Massen-Depolarisationswellen sind gekennzeichnet durch eine außergewöhnlich ausgeprägte Verschiebung von Ionen über die Nervenzellmembran und gehen mit einer starken, anhaltenden Depolarisation einher, welche sich wellenartig in der grauen Substanz ausbreitet. SDs werden regelhaft in vielen akuten Krankheitsbildern des Gehirns angetroffen und gelten allgemein als der zugrunde liegende Mechanismus der Migräne-Aura. Mutationen in ATP1A2, dem humanen Gen, das für die α2-Isoform der Na⁺/K⁺-ATPase kodiert, wurden bei Patienten gefunden, die an einer schweren Form der Migräne mit Aura leiden, der familiären hemiplegischen Migräne Typ 2 (FHM2). Diese Verbindung weist auf eine mögliche Rolle der α2-Isoform in der Entwicklung von SD hin. Trotz Bemühungen die Funktion der α2-Isoform in Knockin-Mausmodellen zu erforschen, ist nur wenig über die Rolle der anderen beiden α-Isoformen bekannt, die im Gehirn exprimiert werden. In der vorliegenden Arbeit habe ich die Rolle dieser drei Na⁺/K⁺-ATPase α-Isoformen mittels dreier verschiedener Knockout-Mauslinien untersucht. Dafür haben wir unter gleichbleibenden Bedingungen die genetische Reduktion von α1 (ubiquitär), α2 (astrozytär) und α3 (neuronal) mit pharmakologischer Hemmung kombiniert und die resultierenden SD-Phänotypen miteinander verglichen. Wir konnten zeigen, dass einzig die Reduktion der α2-Isoform zu einer Erhöhung der Empfänglichkeit für SD führte. Interessanterweise war dieser Effekt abhängig von einer erhöhten extrazellulären K⁺-Konzentration [K⁺]_o und verschwand unter normalen Bedingungen. Darüber hinaus fanden wir heraus, dass die Fähigkeit zur extrazellulären K⁺-Pufferung während intensiver neuronaler Stimulation in α2-heterozygoten Mäusen nahezu unberührt blieb. Wir fanden auch Hinweise für eine Modulierung des zerebralen Gefäßtonus durch die Na⁺/K⁺-ATPase-α2-Isoform, die in einer verstärkten Ausbildung der Post-SD-Hypoperfusion resultierte und in α1- sowie α3-Heterozygoten nicht nachweisbar war. Im Gegensatz dazu konnten wir nachweisen, dass α3-haploinsuffiziente Tiere eine erhöhte Widerstandsfähigkeit gegenüber elektrisch ausgelöster SD aufwiesen, Tiere mit einem Mangel an α1-Isoform jedoch keinerlei Veränderungen des SD-Phänotyps zeigten. Die vorliegenden Ergebnisse sprechen für

eine zentrale Rolle der $\alpha 2$ -Isoform in der Modulation von SD-Empfänglichkeit und der assoziierten Blutflussregulation. Diese Spezifität ist am ehesten auf die funktionelle Kopplung mit sekundär aktiven Transportern zurückzuführen. Insbesondere der beobachtete Blutfluss-Effekt ist im Hinblick auf die Krankheitsbilder Migräne und Schlaganfall von Bedeutung und rechtfertigt eine weitere Abklärung zugrundeliegender Mechanismen.

4. Synopsis

4.1 Introduction

General Introduction

Spreading depolarization (SD) is increasingly recognized as integral part of the neuropathophysiological spectrum of responses observed in acute medical conditions of the human brain.¹ SDs are frequently encountered in the course of ischemic stroke, global ischemia, intracerebral hemorrhage, traumatic brain injury, and subarachnoid hemorrhage (SAH) by means of advanced neuromonitoring in neurocritical care.² Moreover, SD is widely accepted as the underlying mechanism of migraine aura.³ In metabolically compromised brain tissue, SDs are associated with neuronal death⁴ and have been associated with a worsening of the outcome in stroke models, such as the enlargement of the infarction volume.⁵ A striking, inverse vascular response, termed spreading ischemia (SI),^{6,7} accompanies SD under specific pathological conditions and has been shown to cause widespread cortical infarcts in patients with SAH.⁸ The association of SD occurrence with poor clinical outcome and the frequent severe disability and loss of independence in survivors has put SD in the limelight of clinical and basic research. While SD has started as a mere artifact in electrophysiology experiments in the last century,⁹ it has become the subject of extensive basic and clinical research in recent years. However, despite considerable research efforts, it remains unclear whether and how to target SDs therapeutically and under which conditions the outcome of patients can be improved. Furthermore, owing to the complexity of the interplay of neuronal, astrocytic and vascular cells during SD, basic mechanisms are not yet well understood. In this work we aimed at elucidating the role of the Na⁺/K⁺-ATPase in SD, an electrogenic transmembrane ATPase, that is essential for cell survival and neuronal excitability and that plays a fundamental role in the cellular mechanisms of SD.¹⁰

Mechanisms of Spreading Depolarization

On the cellular level, SD is characterized by massive, unparalleled redistribution of ions across cell membranes that causes widespread, sustained neuronal depolarization and propagates as a wave through the gray matter of the central nervous system at a rate of ~2-9 mm/min.¹⁰ Restoration of ion concentration gradients in the wake of SD requires energy-dependent ion translocation across cell membranes that is primarily driven by the Na⁺/K⁺-ATPase. The Na⁺/K⁺-ATPase (sodium-potassium adenosine

triphosphatase, sodium pump) is an essential molecular transporter that accounts for the majority of the energy consumption in the mammalian central nervous system.¹¹ While the pump's energy expenditure is already unmatched under normal conditions, during and following the breakdown of the ionic concentration gradients during SD, increased Na⁺/K⁺-ATPase activity entails even greater demand for ATP.¹² This surge in activity is evidenced by a decrease of the available tissue oxygen, aggravating the supply-demand mismatch.¹³ Conversely, when the tissue falls short of oxygen and oxidizable substrate, such as under ischemic conditions, decreased ATP formation slows Na⁺/K⁺-ATPase turnover and results in protracted re-establishment of ion concentration gradients and membrane repolarization during SD. Accordingly, a gradient of different degrees of depolarization can be observed in stroke that corresponds to the level of metabolic compromise of the tissue surrounding the ischemic core.^{1, 14}

The Na⁺/K⁺-ATPase and Spreading Depolarization

Pharmacological Na⁺/K⁺-ATPase inhibition using cardiac glycosides, such as ouabain, is known to increase the susceptibility to SD and to trigger full-blown SDs at higher concentrations.¹⁵ Interestingly, a specific Na⁺/K⁺-ATPase α isoform has been implicated in an autosomal dominant variant of migraine with aura: Missense mutations in ATP1A2, the gene encoding for the α 2 isoform of the Na⁺/K⁺-ATPase, have been identified in patients suffering from familial hemiplegic migraine type 2 (FHM2).¹⁶ Since SD is believed to be the cellular mechanism underlying migraine aura, animal models of familial hemiplegic migraine have been investigated with regard to their propensity to produce SDs. Indeed, knock-in mouse models of familial hemiplegic migraine type 1 (FHM1) and FHM2 have been demonstrated with elevated SD susceptibility, thereby strengthening the causal link between SD and migraine.^{17, 18} Despite this association, the connection of SD and the pain component of migraine remains controversial.¹⁹ Regardless of the research related to familial hemiplegic migraine with the primary focus on α 2 knock-in mouse models, only little is known about the role of the other two α isoforms of the Na⁺/K⁺-ATPase expressed in the brain. On the basis of the intimate involvement of the Na⁺/K⁺-ATPase in the process of SD, this work aimed at elucidating the role of the three distinct Na⁺/K⁺-ATPase α isoforms in SD: α 1, α 2 and α 3.

The Na⁺/K⁺-ATPase is an integral membrane protein that transports three sodium (Na⁺) ions in exchange for two potassium ions (K⁺) across the plasma membrane during

each cycle of ATP hydrolysis, thereby generating the electrochemical gradient that is essential for neuronal excitability. Moreover, this gradient is vital for the operation of secondary active transporters that mediate the uptake of ions, neurotransmitters and nutrients and that are responsible for regulating cell volume and pH.^{20, 21} The Na⁺/K⁺-ATPase is an oligomer that consists of stoichiometric amounts of α and β subunits. Whereas these two subunits are essential, the association with a third auxiliary protein, termed *gamma subunit* (FXYD protein), is optional. The Na⁺/K⁺-ATPase belongs to the family of the P-type ATPases that change their conformation upon phosphorylation by ATP. It is the α isoform that catalyzes ATP hydrolysis to ADP and binds, occludes and transports Na⁺ and K⁺ across the plasma membrane.^{22, 23} The smaller, highly glycosylated β isoform has been shown to modulate the pump's affinity to Na⁺ and K⁺²⁴ and is involved in correct protein folding and transport of the α isoform to the cell membrane.²⁵

Na⁺/K⁺-ATPase α Isoforms

In the mammalian brain, Na⁺/K⁺-ATPase α isoforms are expressed in three different isoforms, that vary in their expression depending on cell type and developmental stage. Cell-specific expression, different affinities towards cardiac glycosides, heterogeneous expression patterns in the cellular membranes of neurons and astrocytes (*punctate* vs. *homogeneous* distribution), colocalization with different secondary active transporters, and the association of distinct isoforms with human monogenetic disorders suggest distinct functions of the three α isoforms.²⁰ In the adult mammalian brain, the α 2 isoform is predominantly expressed in astrocytes. Its spatial and functional association with the plasmalemmal sodium-calcium exchanger (NCX) is believed to be the basis of the positive inotropic action of cardiac glycosides, such as digoxin, on cardiomyocytes.²⁶ A conceptually similar functional coupling of the α 2 isoform with secondary active transporters has been proposed to drive calcium transporters and presynaptically-released glutamate reuptake into astrocytes.²⁷⁻²⁹ Interestingly, a switch of the cellular expression during early development shifts α 2 expression from neuronal to primarily astrocytic. It has been proposed that predominant neuronal expression at the time of birth is the reason for absence of spontaneous breathing rhythm in brainstem respiratory neurons of homozygous α 2-deficient mice.³⁰ The α 3 isoform is exclusively expressed in neurons in the adult brain. Mutations in ATP1A3, the gene encoding for the α 3 subunit, have been identified in patients suffering from rapid-onset dystonia parkinsonism (RODP), alternating hemiplegia of the childhood (AHC), and in patients with the CAPOS

syndrome (cerebellar ataxia, areflexia, pes cavus, optic atrophy, sensorineural hearing loss). Similar to the $\alpha 2$ isoform, it is expressed in clusters in the cell membrane suggesting a role in fueling secondary active transporters for which it creates local concentrations gradients of Na^+ and K^+ in *membrane microdomains*. The $\alpha 1$ isoform is expressed in all cell types and is assumed to serve as the *housekeeping isoform*. Its expression pattern differs from the $\alpha 2$ and $\alpha 3$ isoform in that it is evenly distributed over the cell membrane as opposed to the punctate pattern observed in the other isoforms. In rodents, the affinity of the endogenous ligand ouabain is ~ 1000 -fold lower for $\alpha 1$ compared to $\alpha 2$ and $\alpha 3$ and as a result, ouabain (g-strophanthin), a compound belonging to the family of the cardenolides, allows for separation of the $\alpha 2/3$ component from the $\alpha 1$ portion of the overall Na^+/K^+ -ATPase activity.²⁰ One of the important roles of the Na^+/K^+ -ATPase in the brain is the clearance of activity-evoked $[\text{K}^+]_o$ transients for which the astrocytic isoform ($\alpha 2$) has been proposed to be the most suited due to its unique kinetic properties. In particular a subunit combination of the $\alpha 2$ and $\beta 2$ isoform that displays a relatively low Na^+ affinity as well as a steep membrane voltage dependence, seems to be geared for removal of activity-induced rises of $[\text{K}^+]_o$.²⁴

Research Questions

This work aimed to address the following main questions:

1. How does $\alpha 2$ deficiency affect the SD phenotype?
2. Does a knock-out model of full $\alpha 2$ haploinsufficiency replicate findings in FHM2 knock-in mouse models of a high SD susceptibility phenotype?
3. Is a potential $\alpha 2$ effect specific for this isoform or can it be reproduced by genetic reduction of the other two brain-expressed isoforms ($\alpha 1$ or $\alpha 3$)?
4. Is a potentially increased SD susceptibility effect mediated by compromised $[\text{K}^+]_o$ clearance?
5. Which of the three brain-expressed Na^+/K^+ -ATPase α isoforms mediates the known facilitating effect of the cardiac glycoside ouabain on SD?
6. Does α isoform deficiency affect the vascular response during SD?

Experimental approach

In the past, the lack of selectivity of the pharmacological approach of utilizing cardiac glycosides precluded an assessment of the individual contribution of the $\alpha 2$ and $\alpha 3$ isoform owing to their similar affinity to the inhibitors. In this work, we have used three

lines of genetically engineered knock-out mice, each heterozygous for one of the three Na⁺/K⁺-ATPase α isoforms expressed in the brain. Heterozygous mice were used because homozygosity for each of the three isoforms results in embryonic (α 1) or neonatal (α 2, α 3) lethality. In addition, we have combined measurements in acute brain slices with and without ouabain to compare pharmacological and genetic reduction of the Na⁺/K⁺-ATPase activity. In order to distinguish neuronal or astroglial effects from vascular effects, we compared measurements in the acute brain slice preparation to in-vivo recordings under two different anesthetic regimens.

4.2 Methods

K⁺-selective microelectrodes

To assess changes in field potential and [K⁺]_o in acute brain slices and in vivo, we employed K⁺-sensitive/reference microelectrodes that we positioned ~100 μ m below the tissue surface.³¹ The pipettes were pulled from double-barreled (theta) glass using a custom-made vertical pipette puller or a Flaming/Brown micropipette puller (P-97, Sutter Instrument) and the tips were broken to ~7.5 μ m diameter. The reference barrel was filled with 154 mM NaCl solution whereas the ion-selective side was repeatedly treated with 5% trimethyl-1 chlorosilane in 95% CCl₄ to ensure adhesion of the potassium ion exchanger resin, which was sucked into the very tip of the microelectrode. Both barrels were equipped with Ag/AgCl wires (200 μ m diameter) and were connected to the difference amplifier headstage. Only electrodes that yielded a potential shift of 59 \pm 1 mV for a 10-fold concentration change (3, 30 mM K⁺) at ~25 °C were accepted for measurement. [K⁺]_o was calculated using a modified Nernst equation:³² $\log_{10}([ION]_a) = E / (s * v) + \log_{10}([ION]_r)$, with E: recorded potential; s: electrode slope obtained at calibration; v: valence of the measured ion; [ION]_r: extracellular ion concentration at rest; [ION]_a: ion concentration at activation.

Intrinsic Optical Signals (IOS)

SD propagation speed and extent of spread in acute brain slices were assessed using light transmittance changes of the tissue.³¹ In the interface-type of recording chamber, SD is associated with a long-lasting decrease in light transmittance that correlates well with the change of other variables, such as the prominent negativity of the extracellular DC-shift, the surge of [K⁺]_o and the precipitous decline in [Na⁺] and [Ca²⁺]. It

is therefore a simple way to assess spatio-temporal features of SD propagation, since it does not require any treatment (fluorescent dye, etc.). To this end, slices rested on 0.4 μm culture plate inserts and were illuminated continuously from below using a cold light source. The changes in light transmittance (AKA intrinsic optical signal, IOS) were recorded with a microscope-mounted CCD camera. We defined the IOS as $\Delta T = ((T_1 - T_0) / T_0) * 100$ to obtain the normalized light transmittance change from baseline in percent, where T_1 and T_0 are transmitted light intensity of a region of interest in the field of view at the time point of interest and 30 s before SD onset, respectively. Single frames were acquired at a rate of 5 Hz and stored for off-line analysis. The speed of SDs was calculated by dividing the propagated distance as indicated by the SD wavefront by the elapsed time. The propagated area was calculated from the two-dimensional projection of the cumulative extent of SD spread indicated by pixels that exceeded 3% from baseline.

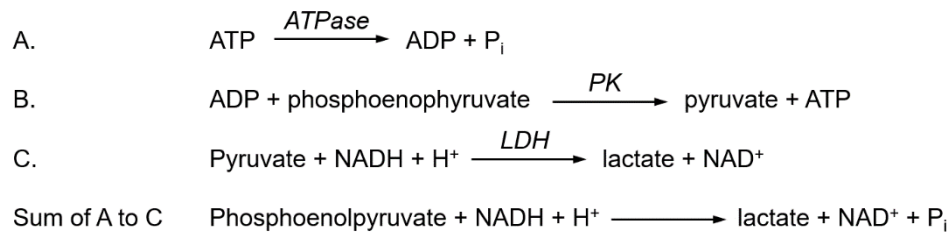
Assessment of $[\text{K}^+]_o$ clearance

To evaluate $[\text{K}^+]_o$ clearance after intense neuronal stimulation in $\alpha 2$ -deficient and wild-type mice, stimulus trains of increasing intensity were applied to the Schaffer collateral pathway in the CA3 subfield of the hippocampus of horizontal acute brain slices with preserved hippocampal circuitry.³¹ To ensure similar stimulation efficacy in all experiments, stimulation intensities were adjusted to yield 25, 50, 75, and 100% of the maximal population spike amplitudes. Stimulus trains (20 Hz, 10 s duration, 100 μs single pulse length) were applied through bipolar stimulation electrodes (platinum wire, 25 μm diameter, 100 μm tip separation). We recorded stimulus-induced changes in $[\text{K}^+]_o$, orthodromic excitatory postsynaptic potentials in stratum radiatum and population spikes in stratum pyramidale using ion-selective/reference microelectrodes. We defined rise time as time elapsed from the start of the stimulus train to 1-1/e of the $[\text{K}^+]_o$ amplitude. The decay time was defined as time elapsed from termination of the stimulus train until $[\text{K}^+]_o$ decay to 1/e of its maximal amplitude.

Na^+/K^+ -ATPase activity assay

To determine actual Na^+/K^+ -ATPase activity in the brains of α isoform knockout mice and their wild-type littermates, we performed a real-time coupled enzyme assay under temperature-controlled conditions.^{31, 33} In the enzyme assay, formation of adenosine diphosphate (ADP) by ATPases is coupled to nicotinamide adenine dinucleotide (NADH)

oxidation in the presence of excess pyruvatekinase (PK), lactatedehydrogenase (LDH), and phosphoenolpyruvate (PEP):³³



The rate of steady-state ATP hydrolysis is proportional to NADH absorbance decrease, measured spectrophotometrically at 340 nm in the presence and absence of two different concentrations of ouabain. The ATPase activity was calculated from the slope of the linear absorption decrease, the NADH millimolar extinction coefficient, the volume of the reaction mixture, and the total amount of protein in the reaction mixture ³³:

$$\text{ATPase activity } (\mu\text{mol P}_i / \text{mg} \cdot \text{h}) = \frac{\text{slope (ODU/h)}}{6.22 \left(\frac{(\text{ODU} \cdot \text{ml})}{(\mu\text{mol})} \right)} \cdot \frac{\text{volume (ml)}}{\text{protein (mg)}}$$

Na⁺/K⁺-ATPase activity corresponds to the portion of total ATPase activity that is suppressible by ouabain. Based on the ~1000-fold lower affinity of the α1 isoform compared to α2 and α3, it is possible to distinguish between both fractions of the Na⁺/K⁺-ATPase activity by adding 10 mM or 10 μM to the reaction mixture. A standard homogenate was prepared from forebrains of C57BL/6J mice and was run with all measurements, mainly to correct for temperature effects. Brains of α2 and α3 knock-out mice and their wild-type littermates were quickly removed and transferred into carbogenated (5% CO₂ and 95% O₂), ice-cold ACSF. The ACSF contained (in mmol/L) 129 NaCl, 3 KCl, 1.8 MgSO₄, 1.6 CaCl₂, 1.25 NaH₂PO₄, 21 NaHCO₃, and 10 glucose (pH 7.4). Forebrains were transferred immediately in liquid nitrogen, omitting the cerebellum. The brain tissue was homogenized in 10 ml solution per 1 g wet weight containing 0.25 M sucrose, 1.25 mM EGTA, and 10 mM Tris, pH 7.0, at 25 °C, using eight strokes in a precooled PTFE-glass Potter-Elvehjem homogenizer. The brain homogenate was then centrifuged at 750 g for 5 minutes (4 °C). We performed analysis of Na⁺/K⁺-ATPase activity on the supernatant without further dilution. Stock solutions of reaction buffer (with 10 μM, 10 mM or without ouabain), auxiliary enzymes and substrates were prepared in

advance. The final reaction mixture contained 125 mM Tris buffer, 1 mM EGTA, 120 mM NaCl, 12.5 mM KCl, 5 mM NaN₃, 5 mM MgCl₂, 5 mM ATP, 2.5 mM phosphoenolpyruvate, 0.5 mM NADH and 15 units each of LDH (type XI) and PK (type III). Brain homogenate samples, auxiliary enzymes and substrates were added to the reaction buffer stock solutions omitting only ATP. The mixture was preincubated 5 min at 37 °C in the reading compartment of a temperature controlled multiwell plate reader. To initiate the reaction 10 µl of ATP-Na₂ solution was added to each well using a reagent injector to assure a constant temperature of 37 °C from the beginning of the reaction. A standard was run simultaneously with the samples. Protein concentration was determined with Bradford Reagent and bovine serum albumin as a standard.

Elevated baseline [K⁺]_o threshold for SD induction

The SD threshold was determined by raising the potassium concentration in the ACSF ([K⁺]_{ACSF}) of coronal brain slices in steps of 2.5 mM at 30-min intervals, starting from 10 mM.³¹ The high [K⁺]_o solution was made by an equimolar replacement of KCl for NaCl. Field potential and threshold [K⁺]_o were recorded by placing an ion-sensitive/reference microelectrode (ISME) in neocortical layer 2/3 in a dorsal position and a second ISME ventral of the rhinal fissure. A different slice from the same animal served to assess pharmacological inhibition by adding 5 µM ouabain to the ACSF. SD threshold was defined as the [K⁺]_o at the time point of the first SD occurrence measured by two ISMEs. The duration of SD's negative direct current (DC) shift was assessed at 25% of the maximum DC shift amplitude. SD latency was defined as the time elapsed between the high [K⁺]_o wash-in until the onset of the first SD.

Microinjection protocol

To assess the SD threshold under normal [K⁺]_o in acute brain slices, SD was triggered focally by injecting small amounts of 1 M KCl solution into the neocortex of transverse brain slices from α2^{+/KOE4} and α2^{+/+} mice.³¹ Micropipettes were pulled from borosilicate glass capillaries and the tip was broken back to a diameter of ~7.0-7.5 µm. KCl-filled pipettes were connected to a pressure ejection system which was adjusted to produce a pressure output of 1 bar. The tip of the pipette was inserted into the tissue to yield a depth of ~100 µm. Pressure pulses of exponentially increasing duration (20, 40, 75, 140, 250, 430, 680, 1000 ms) were applied at 120 s intervals until SD was triggered. Two recording

electrodes were placed in neocortical layer 2/3 ~1.5 mm medial and dorsal from the injection site.

SD threshold and rCBF in vivo (isoflurane anesthesia)

Mice were anesthetized with isoflurane during the surgical procedure and the experiment.³¹ The isoflurane concentration was 4% during anesthesia induction, 2% during the surgical procedure and then adjusted to yield a burst-suppression pattern employing the ECoG recording of spontaneous activity during the SD induction protocol and the recording (1.2%-1.6% isoflurane in 30 ml/min N₂O and 15 ml/min O₂). The mice were placed in a stereotaxic frame, a midline incision was made in the scalp, and the eyes were covered with ointment containing 5% dexpanthenol to reduce drying of the eyes. Two holes were drilled over the right hemisphere, one for the stimulation electrode (diameter 1.3 mm, posterior 2.6 mm, lateral 1.5 mm from bregma) and another smaller one for recording of the epidural ECoG (diameter 0.5 mm, anterior 1 mm, lateral 2 mm from bregma). The stimulation site on the intact dura was covered with a thin film of mineral oil to reduce tissue drying. Regional cerebral perfusion of both hemispheres was monitored during preparation and recording using laser speckle contrast analysis (LASCA) imaging. The near infrared (785 nm) laser allowed for assessment of perfusion (imaging area: 1.3 x 1.1 cm, sampling rate: 0.5 Hz, spatial resolution: 20 μ m, averaged frames per image: 8) through the intact mouse skull and permitted the detection of premature SDs during the preparation phase. Animals with accidentally initiated SDs were excluded from the analysis. SD was induced electrically by applying biphasic pulses of 200 ms (\pm 100 ms) duration with exponentially increasing intensities (20, 30, 40, 50, 60, 80, 100, 150, 200, 260, 340, 450, 600, 800, 1000 mA) at 5-min intervals until SD was triggered. The SD threshold was defined as the smallest electrical charge (electric current [A] * time [s]) necessary to trigger SD. A mains-operated stimulus isolator was employed to ensure a consistent compliance voltage of 100 V. Animals were killed after the experiment by decapitation under 6% isoflurane.

Data analysis and statistical inference

In-vivo experiments with urethane/ α -chloralose anesthesia were randomized and blinded (randomization script in R).³¹ In-vivo experiments with isoflurane as well as brain slice experiments were not blinded. To minimize the effects of subjective bias during analysis, experimental datasets were processed in batches without emphasis on a single

experiment or group and whenever possible, custom scripts (Python, MATLAB™, R) were used to iterate over all files in a data folder. In-vivo experiments using LASCA were only accepted when premature SDs were absent during preparation, as evidenced by similar perfusion levels of both hemispheres and the typical multiphasic rCBF response of the first SD.³⁴ The experimental unit for all descriptive statistics and statistical testing was the single animal, not a brain slice or an event. When several brain slices from the same animal were analyzed, the mean of the measurements was calculated. Two groups were compared using the Mann-Whitney U test. A significance level of $P < 0.05$ was considered statistically significant.

4.3 Results

Genetic $\alpha 2$ isoform reduction increases SD susceptibility under high $[K^+]_o$ baseline in acute brain slices

In order to quantify SD susceptibility in a model of full $\alpha 2$ haploinsufficiency, we employed a protocol of stepwise increasing baseline $[K^+]_o$ in the bathing medium (ACSF) of acute brain slices from $\alpha 2^{+/KOE4}$ mice until SD was triggered. We found a significantly lower threshold $[K^+]_o$ to trigger SD in $\alpha^{+/KOE4}$ mice under elevated baseline $[K^+]_o$ compared to $\alpha^{+/+}$ (wild-type control) mice which was also reflected in a reduction of the latency to SD initiation. Interestingly, the observed threshold and latency effects were of similar magnitude as pharmacological inhibition of the $\alpha 2/3$ portion of the Na^+/K^+ -ATPase with 5 $\mu\text{mol/L}$ ouabain (threshold/latency: $\alpha 2^{+/KOE4}$, -12.7%/-22.2%; ouabain, -16.4%/-22.6%). Lowering of the SD threshold conforms to published data from FHM2 *knock-in* mouse studies that reported increased SD susceptibility in acute brain slices and in vivo.^{17, 28}

Deficiency of the Na^+/K^+ -ATPase $\alpha 1$ or $\alpha 3$ isoform does not impact SD susceptibility under elevated baseline $[K^+]$

One of the central questions of this study was whether a high SD susceptibility phenotype is specific for a deficiency of the Na^+/K^+ -ATPase $\alpha 2$ isoform or, alternatively, whether genetic reduction of the other two brain-expressed α isoforms affects the SD threshold in a similar manner. To address this question, we exposed acute brain slices from $\alpha 1$ - and $\alpha 3$ -deficient mice to the same high baseline $[K^+]$ protocol that was used for acute brain slices from the $\alpha 2$ knock-out mice. In short, we found no effect of genetic $\alpha 1$ or $\alpha 3$ reduction on SD susceptibility in acute brain slices, indicated by similar threshold

[K⁺] and latencies until SD induction. These observations suggest a distinct role of the $\alpha 2$ isoform in modulating SD susceptibility that is not replicated by the other two brain-expressed isoforms.

The clearance of extracellular K⁺ during intense neuronal activation is not altered significantly in $\alpha 2^{+/KOE4}$ mice

To further investigate the underlying mechanistical basis of the increased SD susceptibility in $\alpha 2^{+/KOE4}$ mice under high baseline [K⁺]_o, we assessed measures of extracellular K⁺ clearance after intense neuronal stimulation. In transverse acute brain slices, we stimulated axons forming the Schaffer collateral pathway in the CA3 subfield of the hippocampus and recorded field excitatory postsynaptic potentials, population spikes and changes in [K⁺]_o CA1. We found no impairment of extracellular K⁺ clearance as assessed by the rise time, decay time and peak amplitude of the associated [K⁺]_o surges. Furthermore, undershoots of [K⁺]_o, that have been attributed to post-stimulation Na⁺/K⁺-ATPase activation, did not differ significantly between $\alpha 2^{+/KOE4}$ and $\alpha 2^{+/+}$ mice. These results demonstrate that deficiency of the Na⁺/K⁺-ATPase $\alpha 2$ isoform in $\alpha 2^{+/KOE4}$ mice does not affect K⁺ clearance after intense neuronal activation under normal [K⁺]_o (3 mmol/L).

Under physiological [K⁺]_o, $\alpha 2^{+/KOE4}$ mice display similar resistance against SD compared to wild-type

To assess the effect of genetic $\alpha 2$ reduction on SD susceptibility under physiological [K⁺]_o of 3 mmol/L as opposed to exposure to elevated baseline [K⁺]_o as in the first set of experiments, we induced SD in acute brain slices focally, employing a microinjection protocol. We determined the SD threshold by injecting highly concentrated KCl solution (2 mol/L) into the tissue, stepwise increasing the duration until SD was triggered. In stark contrast to the protocol of increasing baseline [K⁺]_o under normal [K⁺]_o, $\alpha 2^{+/KOE4}$ mice displayed a similar susceptibility to SD compared to their wild-type littermates in the acute brain slice preparation. Furthermore, neither SD speed nor SD extent of spread, calculated from the SD-associated light transmission changes, were significantly different between $\alpha 2^{+/KOE4}$ and $\alpha 2^{+/+}$. Interestingly, we could identify significantly different SD speeds between a dorsal and ventral component of the mouse cortex. This was a consistent observation across all three tested mouse lines and varying slicing planes (transverse, coronal). Unlike $\alpha 2$ deficiency, pharmacological Na⁺/K⁺-ATPase inhibition by bath application of ouabain (5 μ mol/L) drastically increased SD speed and enlarged the

projected area of SD spread. These results point towards key differences of the *knock-out* mouse model of full $\alpha 2$ haploinsufficiency used in this study compared with FHM2 *knock-in* mouse models.

Effects of Na⁺/K⁺-ATPase α isoform deficiency studied in vivo under urethane/ α -chloralose and isoflurane anesthesia

In order to examine the SD threshold effects in the intact organism with preserved neuronal connectivity and in presence of functional vasculature, we performed in-vivo experiments in $\alpha 1^{+/KOE15}$, $\alpha 2^{+/KOE4}$, $\alpha 3^{+/KOI4}$ and the respective wild-type littermates. The first set of experiments was done using intraperitoneally-injected urethane/ α -chloralose to achieve general anesthesia. In a second set of experiments, we employed isoflurane anesthesia and focused in particular on cerebral perfusion. To this end we started LASCA imaging at the time of the preparation of the stimulation site and the ECoG electrode in order to identify premature SDs. Confirming our previous results in acute brain slices under normal $[K^+]_o$ (3 mmol/L), $\alpha 2^{+/KOE4}$ mice displayed a similar SD susceptibility under both anesthetic regimen when compared to $\alpha 2^{+/+}$ mice. Similarly, deficiency of the $\alpha 1$ isoform ($\alpha 1^{+/KOE15}$ mice) did not have an effect on SD threshold or SD speed. By contrast, $\alpha 3^{+/KOI4}$ mice displayed increased resistance to electrical SD induction under urethane/ α -chloralose.

Depression of spontaneous activity following SD in $\alpha 2$ - and $\alpha 3$ -deficient mice

Depression of spontaneous activity, that is associated with SD in electrically active gray matter, is known as spreading depression. In order to quantify the degree of depression during SD, we determined the EEG suppression in the frequency band that was most affected by SD (1-4 Hz). Interestingly, we found the root mean square (RMS) amplitude to be significantly reduced in both $\alpha 2^{+/KOE4}$ and $\alpha 3^{+/KOI4}$ mice compared to their wild-type littermates. This unexpected finding indicates that deficiency of both $\alpha 2$ and $\alpha 3$ isoforms impairs the ability to recover from spreading depression compared to their wild-type littermates.

Marked hypoperfusion in $\alpha 2^{+/KOE4}$ mice under urethane/ α -chloralose anesthesia

Mice have been reported to display a unique rCBF response to SD which is characterized by a long-lasting hypoperfusion that begins in the wake of the “first” SD.³⁴ To assess a possible role of Na⁺/K⁺-ATPase α isoforms in the blood flow response we monitored the hemodynamic response during SDs using laser Doppler flowmetry (LDF)

and, in a later set of experiments, LASCA imaging. Whereas the blood flow response was comparable to wild-type mice in $\alpha 1^{+/KOE15}$ and $\alpha 3^{+/KOE14}$ mice, $\alpha 2^{+/KOE4}$ mice showed an over 30% more pronounced hypoperfusion compared to their wild-type littermates. This effect was evident in both the initial hypoperfusion dip as well as in the long-lasting oligemia following SD. These findings suggest a specific role of the $\alpha 2$ isoform of the Na^+/K^+ -ATPase in regulating cerebral vasculature.

4.4 Discussion

The unique SD phenotypes observed in mouse models of this study indicate distinct roles for the three different brain-expressed Na^+/K^+ -ATPase α isoforms in SD. Despite their identical fundamental function, i.e. the transport of Na^+ into the cell in exchange for K^+ at the expense of ATP, $\alpha 2$ and $\alpha 3$ appear to exert highly specialized functions which are most likely attributable to their functional coupling to secondary-active transporters, which they fuel by providing the electrochemical gradient in spatially restricted membrane sites (*microdomains*). This contrasts with the $\alpha 1$ isoform, which did not affect the SD phenotype and is commonly considered to provide predominantly *housekeeping* roles.

Here, we report that only deficiency of the $\alpha 2$ isoform in $\alpha 2^{+/KOE4}$ mice results in increased SD susceptibility in the acute brain slice preparation. At first glance, this result is in line with observations from a FHM2 knock-in mouse model that displayed higher SD susceptibility in vivo and in acute brain slices.^{17, 28} By contrast, the threshold effect in brain slices of $\alpha 2^{+/KOE4}$ mice disappeared under normal $[\text{K}^+]_o$ (3 mmol/L). This observation raises questions about the underlying mechanistic basis of the high SD susceptibility phenotype that has been reported as a consequence of point mutations in ATP1A2. According to the current understanding, FHM2 mutations that produce an exchange of a single amino acid in the $\alpha 2$ isoform protein result in functional haploinsufficiency. By contrast, the knock-out mice that were employed in our study have been reported to express *no* mutated $\alpha 2$ isoform protein.²⁶ Even if expression would occur, the translated product would lack ~90% of the original protein and would therefore be deficient of its most essential functional elements, such as the nucleotide-binding (N), the phosphorylation (P), and the actuator (A) domain. Thus $\alpha 2^{+/KOE4}$ mice would be expected to serve as a model of full $\alpha 2$ haploinsufficiency. It is therefore surprising to find a relatively mild SD phenotype in $\alpha 2^{+/KOE4}$ mice compared to a well described FHM2 mouse model, such as $\alpha 2^{+/W887R}$.^{17, 28}

Interestingly, two other knock-out mouse models of $\alpha 2$ display different degrees of functional impairment as a consequence of either N- or C-terminal deletions.³⁵ This phenotypic heterogeneity between FHM2 knock-in mouse models and different Na⁺/K⁺-ATPase $\alpha 2$ isoform knock-out mouse models might, beside differences in the experimental approach, reflect the diverse functional consequences of over 80 human disease-linked FHM2 mutations.²³ Further research is required to elucidate the mechanisms underlying phenotypic differences in models of $\alpha 2$ haploinsufficiency.

By comparing genetic with pharmacological Na⁺/K⁺-ATPase activity reduction, we found evidence that the specific, high affinity inhibitor of the Na⁺/K⁺-ATPase, ouabain, which is also synthesized in the human body acting as an endogenous hormone, exerts its SD threshold effects via the $\alpha 2$ isoform. This is supported by the fact, that ouabain application, in a concentration necessary to inhibit the $\alpha 2/3$ portion of the Na⁺/K⁺-ATPase, in brain slices of $\alpha 2^{+/KOE4}$ mice, did not significantly affect the SD threshold. By contrast, pharmacological Na⁺/K⁺-ATPase inhibition significantly lowered the SD threshold in $\alpha 1^{+/KOE15}$ and $\alpha 3^{+/KO14}$, indicating its action through the unaffected $\alpha 2$ isoform. Based on the potential of endogenous ouabain to regulate Na⁺/K⁺-ATPase activity in the human body, it seems an attractive research goal to further investigate possible roles in regulation of cerebral vascular tone and SD susceptibility.

The observed augmented vascular effect of $\alpha 2$ deficiency in the wake of SD in $\alpha 2^{+/KOE4}$ mice agrees with a recent study that reports enhanced contractility in middle cerebral artery (MCA) of $\alpha 2^{+/G301R}$ knock-in mice.³⁶ This observation is particularly interesting, since migraine itself is an independent risk factor for stroke and FHM1 mouse studies have reported increased infarct sizes and SD propagation into subcortical structures.^{37, 38} Mechanistically, the pronounced post-SD oligemia could be mediated by abnormal intracellular Ca²⁺ handling in either astrocytes or vascular smooth muscle cells (VSMCs), which both abundantly express the Na⁺/K⁺-ATPase $\alpha 2$ isoform. Increased Ca²⁺ release from intracellular stores and colocalization of the plasmalemmal Na⁺/Ca²⁺ (NCX) exchanger with the $\alpha 2$ isoform have been demonstrated in various studies. Advancing the understanding about the hemodynamic response during SD is highly relevant for the above-mentioned clinical context in addition to situations in which an inversion of the normal hemodynamic response is observed, such as during SAH.⁸

Conditions of high baseline $[K^+]_o$, such as we utilized to challenge the Na^+/K^+ -ATPase in acute brain slices of $\alpha 2^{+/KOE4}$ mice, appear appropriate for modeling of clinically relevant scenarios, such as SAH, where lysis of accumulated blood cells results in the release of K^+ and hemoglobin into the subarachnoid space. Incidentally, SAH is associated with spreading ischemia, an inverse hemodynamic response to SD that causes widespread laminar infarcts.³⁹ Furthermore, high baseline $[K^+]_o$ has been demonstrated to induce a decline in Na^+/K^+ -ATPase activity in rodent experiments.⁴⁰ In our experiments, an elevated baseline $[K^+]_o$ challenge revealed the inherent SD phenotype, thereby sharing conceptual similarities with the episodic nature of migraine in FHM2 patients where attacks depend on a combination of genetic predisposition and challenging environmental factors.

Understanding of the underlying mechanisms of SD is essential for the development of strategies that help improve the outcome of patients that suffer from potentially life-threatening conditions of the brain, such as traumatic brain injury, intracerebral spontaneous hematoma, aneurysmal SAH and stroke or cardiac arrest that are more often than not associated with the abundant occurrence of SDs.

4.5 List of abbreviations

ACSF, artificial cerebrospinal fluid; ADP, adenosine diphosphate; $\alpha 1^{+/KOE15}$, heterozygous ATP1A1 knock-out; $\alpha 2^{+/KOE4}$, heterozygous ATP1A2 knockout; $\alpha 3^{+/KOI4}$, heterozygous ATP1A3 knockout; AHC, alternating hemiplegia of the childhood; ATP, adenosine triphosphate; Ca^{2+} , calcium; CAPOS, cerebellar ataxia, areflexia, pes cavus, optic atrophy, and sensorineural hearing loss syndrome; DC, direct current; ECoG, electrocorticography; EEG, electroencephalogram; FHM1, familial hemiplegic migraine type 1; FHM2, familial hemiplegic migraine type 2; GLAST, glutamate aspartate transporter; GLT-1, glutamate transporter 1; ISME, ion-sensitive microelectrode; IOS, intrinsic optical signal; K^{+} , potassium; $[K^{+}]_{ACSF}$, K^{+} concentration of the artificial cerebrospinal fluid; $[K^{+}]_o$, extracellular K^{+} concentration; LASCA, laser speckle contrast analysis; LDF, laser Doppler flowmetry; LDH, lactate dehydrogenase; LT, light transmittance; MCA, middle cerebral artery; Na^{+} , sodium; NADH, nicotinamide adenine dinucleotide; NMDAR, N-methyl-D-aspartate receptor; NCX, plasmalemmal Na^{+}/Ca^{2+} -exchanger; NO, nitric oxide; NOS, nitric oxide synthase; ODU, optical density units; pCO_2 , partial pressure of carbon dioxide; PEP, phosphoenolpyruvate; P_i , inorganic phosphate; PK, pyruvate kinase; rCBF, regional cerebral blood flow; RMS, root mean square; RODP, rapid-onset dystonia parkinsonism; SAH, subarachnoid hemorrhage; SD, spreading depolarization; SI, spreading ischemia; VSMC, vascular smooth muscle cell; WT, wild-type littermate.

4.6 Bibliography

1. Dreier JP and Reiffurth C. The stroke-migraine depolarization continuum. *Neuron*. 2015;86:902-922.
2. Dreier JP, Fabricius M, Ayata C, Sakowitz OW, William Shuttleworth C, Dohmen C, Graf R, Vajkoczy P, Helbok R, Suzuki M, Schiefecker AJ, Major S, Winkler MK, Kang EJ, Milakara D, Oliveira-Ferreira AI, Reiffurth C, Revankar GS, Sugimoto K, Dengler NF, Hecht N, Foreman B, Feyen B, Kondziella D, Friberg CK, Piilgaard H, Rosenthal ES, Westover MB, Maslarova A, Santos E, Hertle D, Sanchez-Porras R, Jewell SL, Balanca B, Platz J, Hinzman JM, Luckl J, Schoknecht K, Scholl M, Drenckhahn C, Feuerstein D, Eriksen N, Horst V, Bretz JS, Jahnke P, Scheel M, Bohner G, Rostrup E, Pakkenberg B, Heinemann U, Claassen J, Carlson AP, Kowoll CM, Lublinsky S, Chassidim Y, Shelef I, Friedman A, Brinker G, Reiner M, Kirov SA, Andrew RD, Farkas E, Guresir E, Vatter H, Chung LS, Brennan KC, Lieutaud T, Marinesco S, Maas AI, Sahuquillo J, Dahlem MA, Richter F, Herreras O, Boutelle MG, Okonkwo DO, Bullock MR, Witte OW, Martus P, van den Maagdenberg AM, Ferrari MD, Dijkhuizen RM, Shutter LA, Andaluz N, Schulte AP, MacVicar B, Watanabe T, Woitzik J, Lauritzen M, Strong AJ and Hartings JA. Recording, analysis, and interpretation of spreading depolarizations in neurointensive care: Review and recommendations of the COSBID research group. *J Cereb Blood Flow Metab*. 2017;37:1595-1625.
3. Lashley KS. Patterns of cerebral integration indicated by the scotomas of migraine. *Arch Neuro Psychiatr*. 1941;46:331-339.
4. Luckl J, Lemale CL, Kola V, Horst V, Khojasteh U, Oliveira-Ferreira AI, Major S, Winkler MKL, Kang EJ, Schoknecht K, Martus P, Hartings JA, Woitzik J and Dreier JP. The negative ultraslow potential, electrophysiological correlate of infarction in the human cortex. *Brain*. 2018;141:1734-1752.
5. Nakamura H, Strong AJ, Dohmen C, Sakowitz OW, Vollmar S, Sue M, Kracht L, Hashemi P, Bhatia R, Yoshimine T, Dreier JP, Dunn AK and Graf R. Spreading depolarizations cycle around and enlarge focal ischaemic brain lesions. *Brain*. 2010;133:1994-2006.
6. Dreier JP, Korner K, Ebert N, Gorner A, Rubin I, Back T, Lindauer U, Wolf T, Villringer A, Einhaupl KM, Lauritzen M and Dirnagl U. Nitric oxide scavenging by

hemoglobin or nitric oxide synthase inhibition by N-nitro-L-arginine induces cortical spreading ischemia when K⁺ is increased in the subarachnoid space. *J Cereb Blood Flow Metab.* 1998;18:978-90.

7. Dreier JP, Ebert N, Priller J, Megow D, Lindauer U, Klee R, Reuter U, Imai Y, Einhaupl KM, Victorov I and Dirnagl U. Products of hemolysis in the subarachnoid space inducing spreading ischemia in the cortex and focal necrosis in rats: a model for delayed ischemic neurological deficits after subarachnoid hemorrhage? *J Neurosurg.* 2000;93:658-66.

8. Dreier JP. The role of spreading depression, spreading depolarization and spreading ischemia in neurological disease. *Nat Med.* 2011;17:439-47.

9. Leao AAP. Spreading depression of activity in the cerebral cortex. *Journal of Neurophysiology.* 1944;7:359-390.

10. Somjen GG. Mechanisms of spreading depression and hypoxic spreading depression-like depolarization. *Physiol Rev.* 2001;81:1065-96.

11. Howarth C, Gleeson P and Attwell D. Updated energy budgets for neural computation in the neocortex and cerebellum. *J Cereb Blood Flow Metab.* 2012;32:1222-32.

12. Dreier JP, Isele T, Reiffurth C, Offenhauser N, Kirov SA, Dahlem MA and Herreras O. Is spreading depolarization characterized by an abrupt, massive release of Gibbs free energy from the human brain cortex? *Neuroscientist.* 2013;19:25-42.

13. von Bornstadt D, Houben T, Seidel JL, Zheng Y, Dilekoz E, Qin T, Sandow N, Kura S, Eikermann-Haerter K, Endres M, Boas DA, Moskowitz MA, Lo EH, Dreier JP, Woitzik J, Sakadzic S and Ayata C. Supply-demand mismatch transients in susceptible peri-infarct hot zones explain the origins of spreading injury depolarizations. *Neuron.* 2015;85:1117-31.

14. Hartings JA, Shuttleworth CW, Kirov SA, Ayata C, Hinzman JM, Foreman B, Andrew RD, Boutelle MG, Brennan KC, Carlson AP, Dahlem MA, Drenckhahn C, Dohmen C, Fabricius M, Farkas E, Feuerstein D, Graf R, Helbok R, Lauritzen M, Major S, Oliveira-Ferreira AI, Richter F, Rosenthal ES, Sakowitz OW, Sanchez-Porrás R, Santos E, Scholl M, Strong AJ, Urbach A, Westover MB, Winkler MK, Witte OW, Woitzik

J and Dreier JP. The continuum of spreading depolarizations in acute cortical lesion development: Examining Leao's legacy. *J Cereb Blood Flow Metab.* 2017;37:1571-1594.

15. Balestrino M, Young J and Aitken P. Block of (Na⁺,K⁺)ATPase with ouabain induces spreading depression-like depolarization in hippocampal slices. *Brain Res.* 1999;838:37-44.

16. De Fusco M, Marconi R, Silvestri L, Atorino L, Rampoldi L, Morgante L, Ballabio A, Aridon P and Casari G. Haploinsufficiency of ATP1A2 encoding the Na⁺/K⁺ pump alpha2 subunit associated with familial hemiplegic migraine type 2. *Nat Genet.* 2003;33:192-6.

17. Leo L, Gherardini L, Barone V, De Fusco M, Pietrobon D, Pizzorusso T and Casari G. Increased susceptibility to cortical spreading depression in the mouse model of familial hemiplegic migraine type 2. *PLoS Genet.* 2011;7:e1002129.

18. Bottger P, Glerup S, Gesslein B, Illarionova NB, Isaksen TJ, Heuck A, Clausen BH, Fuchtbauer EM, Gramsbergen JB, Gunnarson E, Aperia A, Lauritzen M, Lambertsen KL, Nissen P and Lykke-Hartmann K. Glutamate-system defects behind psychiatric manifestations in a familial hemiplegic migraine type 2 disease-mutation mouse model. *Sci Rep.* 2016;6:22047.

19. Brennan KC and Pietrobon D. A Systems Neuroscience Approach to Migraine. *Neuron.* 2018;97:1004-1021.

20. Blanco G and Mercer RW. Isozymes of the Na-K-ATPase: heterogeneity in structure, diversity in function. *Am J Physiol.* 1998;275:F633-50.

21. Skou JC. The Influence of Some Cations on an Adenosine Triphosphatase from Peripheral Nerves. *Biochimica Et Biophysica Acta.* 1957;23:394-401.

22. Morth JP, Pedersen BP, Toustrup-Jensen MS, Sorensen TL, Petersen J, Andersen JP, Vilsen B and Nissen P. Crystal structure of the sodium-potassium pump. *Nature.* 2007;450:1043-9.

23. Friedrich T, Tavraz NN and Junghans C. ATP1A2 Mutations in Migraine: Seeing through the Facets of an Ion Pump onto the Neurobiology of Disease. *Front Physiol.* 2016;7:239.

24. Stoica A, Larsen BR, Assentoft M, Holm R, Holt LM, Vilhardt F, Vilsen B, Lykke-Hartmann K, Olsen ML and MacAulay N. The alpha2beta2 isoform combination dominates the astrocytic Na(+)/K(+)-ATPase activity and is rendered nonfunctional by the alpha2.G301R familial hemiplegic migraine type 2-associated mutation. *Glia*. 2017;65:1777-1793.
25. Chow DC and Forte JG. Functional significance of the beta-subunit for heterodimeric P-type ATPases. *J Exp Biol*. 1995;198:1-17.
26. James PF, Grupp IL, Grupp G, Woo AL, Askew GR, Croyle ML, Walsh RA and Lingrel JB. Identification of a specific role for the Na,K-ATPase alpha 2 isoform as a regulator of calcium in the heart. *Mol Cell*. 1999;3:555-63.
27. Juhaszova M and Blaustein MP. Distinct distribution of different Na⁺ pump alpha subunit isoforms in plasmalemma. Physiological implications. *Ann N Y Acad Sci*. 1997;834:524-36.
28. Capuani C, Melone M, Tottene A, Bragina L, Crivellaro G, Santello M, Casari G, Conti F and Pietrobon D. Defective glutamate and K⁺ clearance by cortical astrocytes in familial hemiplegic migraine type 2. *EMBO Mol Med*. 2016;8:967-86.
29. Golovina VA, Song H, James PF, Lingrel JB and Blaustein MP. Na⁺ pump alpha 2-subunit expression modulates Ca²⁺ signaling. *Am J Physiol Cell Physiol*. 2003;284:C475-86.
30. Ikeda K, Onimaru H, Yamada J, Inoue K, Ueno S, Onaka T, Toyoda H, Arata A, Ishikawa TO, Taketo MM, Fukuda A and Kawakami K. Malfunction of respiratory-related neuronal activity in Na⁺, K⁺-ATPase alpha2 subunit-deficient mice is attributable to abnormal Cl⁻ homeostasis in brainstem neurons. *J Neurosci*. 2004;24:10693-701.
31. Reiffurth C, Alam M, Zahedi-Khorasani M, Major S and Dreier JP. Na(+)/K(+)-ATPase alpha isoform deficiency results in distinct spreading depolarization phenotypes. *J Cereb Blood Flow Metab*. 2019:271678X19833757.
32. Heinemann U, Arens J, Kettenmann H and Grantyn R. Production and calibration of ion-sensitive microelectrodes *Practical electrophysiological methods: a guide for in vitro studies in vertebrate neurobiology* New York: Wiley-Liss; 1992: 206-212.

33. Scharschmidt BF, Keeffe EB, Blankenship NM and Ockner RK. Validation of a Recording Spectrophotometric Method for Measurement of Membrane-Associated Mg- and Na-K-ATPase Activity. *J Lab Clin Med.* 1979;93:790-799.
34. Ayata C, Shin HK, Salomone S, Ozdemir-Gursoy Y, Boas DA, Dunn AK and Moskowitz MA. Pronounced hypoperfusion during spreading depression in mouse cortex. *J Cereb Blood Flow Metab.* 2004;24:1172-82.
35. Uekawa M, Ikeda K, Tomita Y, Kawakami K and Suzuki N. Enhanced susceptibility to cortical spreading depression in two types of Na(+),K(+)-ATPase alpha2 subunit-deficient mice as a model of familial hemiplegic migraine 2. *Cephalalgia.* 2018;38:1515-1524.
36. Staehr C, Hangaard L, Bouzinova EV, Kim S, Rajanathan R, Boegh Jessen P, Luque N, Xie Z, Lykke-Hartmann K, Sandow SL, Aalkjaer C and Matchkov VV. Smooth muscle Ca(2+) sensitization causes hypercontractility of middle cerebral arteries in mice bearing the familial hemiplegic migraine type 2 associated mutation. *J Cereb Blood Flow Metab.* 2018:271678X18761712.
37. Eikermann-Haerter K, Lee JH, Yuzawa I, Liu CH, Zhou Z, Shin HK, Zheng Y, Qin T, Kurth T, Waeber C, Ferrari MD, van den Maagdenberg AM, Moskowitz MA and Ayata C. Migraine mutations increase stroke vulnerability by facilitating ischemic depolarizations. *Circulation.* 2012;125:335-45.
38. Eikermann-Haerter K, Yuzawa I, Qin T, Wang Y, Baek K, Kim YR, Hoffmann U, Dilekoz E, Waeber C, Ferrari MD, van den Maagdenberg AM, Moskowitz MA and Ayata C. Enhanced subcortical spreading depression in familial hemiplegic migraine type 1 mutant mice. *J Neurosci.* 2011;31:5755-63.
39. Dreier JP, Drenckhahn C, Woitzik J, Major S, Offenhauser N, Weber-Carstens S, Wolf S, Strong AJ, Vajkoczy P, Hartings JA and Group CS. Spreading ischemia after aneurysmal subarachnoid hemorrhage. *Acta Neurochir Suppl.* 2013;115:125-9.
40. Major S, Petzold GC, Reiffurth C, Windmuller O, Foddis M, Lindauer U, Kang EJ and Dreier JP. A role of the sodium pump in spreading ischemia in rats. *J Cereb Blood Flow Metab.* 2017;37:1687-1705.

5. Eidesstattliche Versicherung

„Ich, Clemens Reiffurth, versichere an Eides statt durch meine eigenhändige Unterschrift, dass ich die vorgelegte Dissertation mit dem Thema: „The Role of Na⁺/K⁺-ATPase α Isoforms in Spreading Depolarization“ selbstständig und ohne nicht offengelegte Hilfe Dritter verfasst und keine anderen als die angegebenen Quellen und Hilfsmittel genutzt habe.

Alle Stellen, die wörtlich oder dem Sinne nach auf Publikationen oder Vorträgen anderer Autoren beruhen, sind als solche in korrekter Zitierung kenntlich gemacht. Die Abschnitte zu Methodik (insbesondere praktische Arbeiten, Laborbestimmungen, statistische Aufarbeitung) und Resultaten (insbesondere Abbildungen, Graphiken und Tabellen werden von mir verantwortet.

Meine Anteile an etwaigen Publikationen zu dieser Dissertation entsprechen denen, die in der untenstehenden gemeinsamen Erklärung mit dem Betreuer, angegeben sind. Für sämtliche im Rahmen der Dissertation entstandenen Publikationen wurden die Richtlinien des ICMJE (International Committee of Medical Journal Editors; www.icmje.org) zur Autorenschaft eingehalten. Ich erkläre ferner, dass mir die Satzung der Charité – Universitätsmedizin Berlin zur Sicherung Guter Wissenschaftlicher Praxis bekannt ist und ich mich zur Einhaltung dieser Satzung verpflichte.

Die Bedeutung dieser eidesstattlichen Versicherung und die strafrechtlichen Folgen einer unwahren eidesstattlichen Versicherung (§156,161 des Strafgesetzbuches) sind mir bekannt und bewusst.“

Datum

Unterschrift

6. Ausführliche Anteilserklärung

Ausführliche Anteilserklärung an der erfolgten Publikation als Top-Journal im Rahmen der Promotionsverfahren zum PhD bzw. MD/PhD

Publikation: Reiffurth, C., M. Alam, M. Zahedi-Khorasani, S. Major and J. P. Dreier, "Na(+)/K(+)-ATPase α isoform deficiency results in distinct spreading depolarization phenotypes.", J Cereb Blood Flow Metab, February 28, 2019

Beitrag im Einzelnen: Organisation der Zucht und Durchführung der Genotypisierung (PCR, Projektleitung Gentechnik) von $\alpha 1^{+/KOE15}$, $\alpha 2^{+/KOE4}$, $\alpha 3^{+/KOE4}$; Etablierung und Durchführung des spektrophotometrischen Na⁺/K⁺-ATPase-Assays unter temperaturkontrollierten Bedingungen ($\alpha 2^{+/KOE4}$, $\alpha 3^{+/KOE4}$); Anfertigen der ionenselektiven Mikroelektroden für sämtliche Messungen in akuten Hirnschnitten und in vivo; Experimente in akuten Hirnschnitten ($\alpha 1^{+/KOE15}$, $\alpha 2^{+/KOE4}$, $\alpha 3^{+/KOE4}$) mit und ohne Ouabain: High-[K⁺]_o-Protokoll [Abb. 1, 2], Stimulus-induzierte [K⁺]_o-Anstiege [Abb. 3], fokale Mikroinjektion zur SD-Schwellenbestimmung [Abb. 4]; Experimente in vivo ($\alpha 1^{+/KOE15}$, $\alpha 2^{+/KOE4}$, $\alpha 3^{+/KOE4}$): Schwellenbestimmungen unter Isofluran-Anästhesie und regionale Blutflussänderungen mittels LASCA-Imaging [Abb. 5, 6]; Koordination, Supervision inkl. Verblindung der Experimente unter α -Chloralose/Urethan [Abb. 5, 6]; Erstellen von Programmen zur digitalen Signalverarbeitung und Auswertung/Aufnahme der elektrophysiologischen und Bilddaten in MATLAB™, Python, R (Aufnahme von IOS-Zeitreihen; automatisierte Berechnung der Kenngrößen bei Stimulus-induzierten [K⁺]_o-Anstiegen; Berechnung von SD-Geschwindigkeit und -Fläche in Hirnschnitten, SD-assoziierte EEG-Depression mit Fourier-Transformation [Abb. 5i-j], rCBF-Berechnung [Abb. 6], standardmäßige Ausgabe der IOS-Änderung in Hirnschnitten mittels substituierenden Pseudofarben [Abb. 1a, 5d]); Auswertung und Interpretation der Daten, Schreiben des Manuskripts, Erstellen sämtlicher Abbildungen (Abb. 1-6), Revidieren des Manuskripts entsprechend der Vorgaben des Reviewers.

Unterschrift des Doktoranden

7. Excerpt from the Journal Summary List

Journal Data Filtered By: **Selected JCR Year: 2017** Selected Editions: SCIE,SSCI
 Selected Categories: **"NEUROSCIENCES"** Selected Category Scheme: WoS
Gesamtanzahl: 261 Journale

Rank	Full Journal Title	Total Cites	Journal Impact Factor	Elgenfactor Score
1	NATURE REVIEWS NEUROSCIENCE	40,834	32.635	0.069940
2	NATURE NEUROSCIENCE	59,426	19.912	0.153710
3	ACTA NEUROPATHOLOGICA	18,783	15.872	0.041490
4	TRENDS IN COGNITIVE SCIENCES	25,391	15.557	0.040790
5	BEHAVIORAL AND BRAIN SCIENCES	8,900	15.071	0.010130
6	Annual Review of Neuroscience	13,320	14.675	0.016110
7	NEURON	89,410	14.318	0.216730
8	PROGRESS IN NEUROBIOLOGY	13,065	14.163	0.015550
9	BIOLOGICAL PSYCHIATRY	42,494	11.982	0.056910
10	MOLECULAR PSYCHIATRY	18,460	11.640	0.047200
11	JOURNAL OF PINEAL RESEARCH	9,079	11.613	0.008600
12	TRENDS IN NEUROSCIENCES	20,061	11.439	0.026860
13	BRAIN	52,061	10.840	0.075170
14	SLEEP MEDICINE REVIEWS	6,080	10.602	0.010720
15	ANNALS OF NEUROLOGY	37,251	10.244	0.053390
16	Translational Stroke Research	2,202	8.266	0.005260
17	NEUROSCIENCE AND BIOBEHAVIORAL REVIEWS	24,279	8.037	0.048460
18	NEUROSCIENTIST	4,738	7.461	0.008730
19	NEURAL NETWORKS	10,086	7.197	0.015290
20	FRONTIERS IN NEUROENDOCRINOLOGY	3,924	6.875	0.006040
21	NEUROPSYCHOPHARMACOLOGY	24,537	6.544	0.042870
22	CURRENT OPINION IN NEUROBIOLOGY	14,190	6.541	0.034670
23	Molecular Neurodegeneration	3,489	6.426	0.009850
24	CEREBRAL CORTEX	29,570	6.308	0.058970
25	BRAIN BEHAVIOR AND IMMUNITY	12,583	6.306	0.026850
26	BRAIN PATHOLOGY	4,952	6.187	0.007750
27	Brain Stimulation	4,263	6.120	0.014510
28	NEUROPATHOLOGY AND APPLIED NEUROBIOLOGY	3,654	6.059	0.006350
29	JOURNAL OF CEREBRAL BLOOD FLOW AND METABOLISM	19,450	6.045	0.028280
30	JOURNAL OF NEUROSCIENCE	176,157	5.970	0.265950
31	Molecular Autism	1,679	5.872	0.006320
31	Translational Neurodegeneration	589	5.872	0.002280
33	GLIA	13,417	5.846	0.020530
34	Neurotherapeutics	3,973	5.719	0.008980
35	PAIN	36,132	5.559	0.038000
36	NEUROIMAGE	92,719	5.426	0.152610
37	Acta Neuropathologica Communications	2,326	5.414	0.011550
38	Multiple Sclerosis Journal	10,675	5.280	0.021890



8. Print copy of publication

The following copy of the publication, *Reiffurth, C., Alam, M., Zahedi-Khorasani, M., Major, S., and Dreier, J.P. (2019) - Na⁺/K⁺-ATPase α isoform deficiency results in distinct spreading depolarization phenotypes, J Cereb Blood Flow Metab DOI:10.1177/0271678X19833757*, is used under the terms of the Creative Commons Attribution License (CC BY-NC 4.0): <https://creativecommons.org/licenses/by/4.0/>. The final version of this paper has been published in the Journal of Cerebral Blood Flow and Metabolism, volume 40, issue 3, March 1/2020 by SAGE Publications Ltd, all rights reserved. Reiffurth, C., Alam, M., Zahedi-Khorasani, M., Major, S., and Dreier, J.P., 2019. The full text is available at: <https://journals.sagepub.com/home/jcb>.

Na⁺/K⁺-ATPase α isoform deficiency results in distinct spreading depolarization phenotypes

Clemens Reiffurth^{1,2}, Mesbah Alam³, Mahdi Zahedi-Khorasani⁴, Sebastian Major^{1,2,5} and Jens P Dreier^{1,2,5,6,7} 

Journal of Cerebral Blood Flow & Metabolism

2020, Vol. 40(3) 622–638

© Author(s) 2019



Article reuse guidelines:

sagepub.com/journals-permissions

DOI: 10.1177/0271678X19833757

journals.sagepub.com/home/jcbfm



Abstract

Compromised Na⁺/K⁺-ATPase function is associated with the occurrence of spreading depolarization (SD). Mutations in ATP1A2, the gene encoding the α 2 isoform of the Na⁺/K⁺-ATPase, were identified in patients with familial hemiplegic migraine type 2 (FHM2), a Mendelian model disease for SD. This suggests a distinct role for the α 2 isoform in modulating SD susceptibility and raises questions about underlying mechanisms including the roles of other Na⁺/K⁺-ATPase α isoforms. Here, we investigated the effects of genetic ablation and pharmacological inhibition of α 1, α 2, and α 3 on SD using heterozygous knock-out mice. We found that only α 2 heterozygous mice displayed higher SD susceptibility when challenged with prolonged extracellular high potassium concentration ([K⁺]_o), a pronounced post SD oligemia and higher SD speed in-vivo. By contrast, under physiological [K⁺]_o, α 2 heterozygous mice showed similar SD susceptibility compared to wild-type littermates. Deficiency of α 3 resulted in increased resistance against electrically induced SD in-vivo, whereas α 1 deficiency did not affect SD. The results support important roles of the α 2 isoform in SD. Moreover, they suggest that specific experimental conditions can be necessary to reveal an inherent SD phenotype by driving a (meta-) stable system into decompensation, reminiscent of the episodic nature of SDs in various diseases.

Keywords

Spreading depolarization, spreading depression, Na,K-ATPase, familial hemiplegic migraine, knock-out mouse model

Received 5 September 2018; Revised 24 January 2019; Accepted 24 January 2019

Introduction

Spreading depolarization (SD) is the generic term for all waves of abrupt, near-complete breakdown of the neuronal transmembrane ion gradients that cause neuronal edema and propagate at about 3 mm/min in cerebral gray matter. The SD continuum describes the spectrum from short-lasting SD in metabolically intact tissue to SD of intermediate duration to terminal SD in severely ischemic tissue. Accordingly, SDs occur in human diseases from the harmless migraine aura to stroke to circulatory arrest, which means that there are overlaps but also large variations in mechanistic aspects along the SD continuum.^{1,2}

The Na⁺/K⁺-ATPase generates the steep transmembrane gradients of the two principal ions, Na⁺ and K⁺, and accounts for ~50% of the brain's ATP consumption under resting conditions.^{3,4} Accordingly, pharmacological Na⁺/K⁺-ATPase inhibition, using cardiac

¹Department of Experimental Neurology, Charité-University Medicine Berlin, Berlin, Germany

²Center for Stroke Research, Charité-University Medicine Berlin, Berlin, Germany

³Department of Neurosurgery, Hannover Medical School, Hannover, Germany

⁴Research Center and Department of Physiology, School of Medicine, Semnan University of Medical Sciences, Semnan, Iran

⁵Department of Neurology, Charité-University Medicine Berlin, Berlin, Germany

⁶Bernstein Center for Computational Neuroscience Berlin, Berlin, Germany

⁷Einstein Center for Neurosciences Berlin, Berlin, Germany

Corresponding author:

Jens P Dreier, Center for Stroke Research Berlin, Department of Neurology, Department of Experimental Neurology, Charitéplatz 1, Berlin 10117, Germany.

Email: jens.dreier@charite.de

glycosides such as ouabain, is known to trigger SD under normoxic conditions⁵ and SD under anoxia/ischemia is assumed to result from failure of the Na⁺/K⁺-ATPase due to lack of ATP.^{6,7} Three distinct α isoforms of the Na⁺/K⁺-ATPase are expressed in the brain by individual genes in a developmentally regulated and cell-type specific manner: α 1, α 2, and α 3.^{8,9} Na⁺/K⁺-ATPase α isoforms vary in their kinetic properties and in their affinity to Na⁺, K⁺, ATP and ouabain.¹⁰ The α 1 isoform can be found on most cell types and is considered to be the housekeeping enzyme. In the adult brain, the α 2 isoform is expressed predominantly on astrocytes, whereas the α 3 isoform is expressed exclusively on neurons.^{8,11} Experimental data suggest that the α 2 isoform exerts specific functions through coupling to secondary active transporters and functional interaction in spatially restricted microdomains^{12–15} and has been reported to co-localize with glutamate reuptake transporters.^{16,17} Association of mutations in the α 2 and α 3 isoform with neurological disorders suggests isoform-specific functions. Whereas mutations in the gene encoding the α 2 isoform have been identified in patients with FHM2, a severe Mendelian form of migraine with aura,¹⁸ mutations in ATP1A3, the gene coding for the α 3 subunit, are linked to rapid-onset dystonia parkinsonism (RODP),¹⁹ alternating hemiplegia of the childhood (AHC)^{20,21} and cerebellar ataxia, areflexia, pes cavus, optic atrophy, and sensorineural hearing loss (CAPOS) syndrome.²²

Two FHM2 knock-in mouse models (α 2^{+/^{W887R}, α 2^{+/^{G301R}) have been reported to exhibit a high SD susceptibility phenotype^{23,24} and both have been shown to have impaired astrocytic glutamate clearance.^{24,25} However, it is unknown how other Na⁺/K⁺-ATPase α isoforms, in particular the neuronal isoform, modulate the SD process and how their role in SD compares to α 2. A similar affinity of cardiac glycosides to α 2 and α 3 has precluded a pharmacological approach to studying distinct isoforms' function. To investigate the roles of the three Na⁺/K⁺-ATPase α isoforms in SD, we employed mice heterozygous for a null mutation in each of the isoform genes.^{14,26} Because all three Na⁺/K⁺-ATPase α isoforms are essential, homozygosity of the null mutation is embryonically or neonatally lethal. By contrast, heterozygous mice do not have an apparent phenotype and breed normally. In acute brain slices and in-vivo experiments, we investigated the effect of genetic and pharmacological reduction of Na⁺/K⁺-ATPase α isoform activity on SD threshold, propagation and recovery.}}

Materials and methods

Animals

The reporting of animal experiments complies with the ARRIVE Guidelines. All animal experiments were

authorized by the animal welfare authorities in Berlin, Germany: Berlin State Office for Health and Social Affairs (LAGeSo), T0311/11 and G0152-11, and all experimental procedures were conducted in accordance with the Charité Animal Welfare Guidelines.

The effects of genetic reduction of Na⁺/K⁺-ATPase α isoforms on SD were studied in α isoform-deficient knock-out mice ($n=340$) bearing a null mutation in one allele of each of the murine orthologous genes: ATP1A1, ATP1A2, and ATP1A3. All three mouse lines employed in this study were genetically engineered, using techniques of targeted disruption and homologous recombination, at the University of Cincinnati, Ohio, USA.^{14,26} Heterozygous animals did not display an apparent clinical phenotype or histological brain anomalies and were fertile. Na⁺/K⁺-ATPase α isoform-deficient mice were backcrossed to (F>9) and maintained on a C57BL/6J (Jackson Laboratory, Bar Harbor, ME, USA) genetic background. Genotyping was performed by PCR as previously described.^{14,26} Adult male mice, 12–18 weeks of age from each line (α 1, α 2, and α 3 heterozygous and wild-type littermates) were used. Animals were housed in groups (at least two animals per cage) under a 12-h light–dark cycle with food and tap water available ad libitum. Due to the effect of sex hormones on migraine prevalence and SD susceptibility,^{27,28} only male mice were used in this study. To compensate for possible differences in genetic background or environmental factors, heterozygous knock-out mice were only compared to their wild-type littermates (WT).²⁹ For in-vivo experiments, additional confirmatory genotyping was performed.

Na⁺/K⁺-ATPase α isoform-deficient mouse line details

Mice deficient for the α 1 isoform (α 1^{+/^{KOE15}, ATP1A1^{+/^{tm1Ling}) bear a mutation in ATP1A1 that results in removal of exons 15 through 18. Western blot analysis of hippocampal whole tissue extracts revealed a reduction of ~70% of the α 1 isoform with no change in α 2 and α 3 isoform levels.^{14,26} Knock-out mice for α 2 (α 2^{+/^{KOE4}, ATP1A2^{+/^{tm1Ling}) were generated by introducing a deletion in exon 4. Although no transcript was detectable in cardiac homogenates,¹⁴ expression of the protein would result in a truncation of the protein after the first transmembrane domain. Protein expression in hippocampal extracts showed a reduction of α 2 by ~50%, no change in α 1, and α 3 with a ~25% lower expression compared to wild types.²⁶ Mice deficient for the α 3 isoform (α 3^{+/^{KOI4}, ATP1A3^{+/^{tm1Ling}) were generated by introducing a point mutation in intron 4 in ATP1A3, causing aberrant mRNA processing that entails an unstable transcript and loss of expression. Hippocampal protein}}}}}}

expression of $\alpha 3$ was shown to be reduced by $\sim 60\%$, $\alpha 1$ was increased by $\sim 35\%$, and the $\alpha 2$ isoform was unchanged compared to wild types.²⁶

Acute brain slice experiments

Animals ($n = 128$) were deeply anesthetized with isoflurane and decapitated. The brain was quickly removed from the skull and transferred into chilled ($0\text{--}4^\circ\text{C}$) carbogenated (5% CO_2 and 95% O_2) artificial cerebrospinal fluid (ACSF). The ACSF contained (in mmol/L) 129 NaCl, 3 KCl, 1.8 MgSO_4 , 1.6 CaCl_2 , 1.25 NaH_2PO_4 , 21 NaHCO_3 , and 10 glucose (pH 7.4). Depending on the protocol, either coronal or transverse acute brain slices with a thickness of $400\ \mu\text{m}$ were prepared using a vibrating blade microtome (Vibroslice, MA752, Campden Instruments, Loughborough, Leics., England). Brain slices were transferred to an interface-type recording chamber and perfused with prewarmed (36°C) carbogenated ACSF in a humidified atmosphere of 95% $\text{O}_2/5\%$ CO_2 . Before starting the recordings, the tissue was allowed to equilibrate for $\sim 60\ \text{min}$.^{30–32} Viability was assessed by stimulating at the boundary of layer VI to the subjacent white matter using a bipolar platinum stimulation electrode (diameter $25\ \mu\text{m}$, tip separation $100\ \mu\text{m}$, single-pulse duration $100\ \mu\text{s}$, intensity $5\text{--}10\ \text{V}$) and recording field potentials in neocortical layers II/III. In horizontal slices, stimulation of the Schaffer collateral pathway in the hippocampus resulted in a population spike (PS) in stratum pyramidale of the CA1 which was used instead. Slices were accepted if stimulation resulted in a field potential amplitude of at least $1.5\ \text{mV}$. Recorded potential changes were amplified (custom-built ISME amplifier), field potentials were low-pass filtered at $3\ \text{kHz}$ and sampled at $10\ \text{kHz}$, ion-selective potentials were low-pass filtered at $30\ \text{Hz}$ and sampled at $100\ \text{Hz}$, displayed on an oscilloscope, digitized (CED-1401, Spike2 software; Cambridge Electronic Design Limited, Milton, Cambridge, England), and stored for off-line analysis. Electrical stimulation pulses were generated using a programmable pulse generator (Master-8, AMPI Instruments, Jerusalem, Israel) connected to a stimulus-isolator (BSI-1, BAK Electronics, Umatilla, FL, USA).

In-vivo: Urethane/ α -chloralose anesthesia

Heterozygous knock-out mice ($n = 73$) were anesthetized with intraperitoneal injection of urethane ($600\ \text{mg/kg}$) and α -chloralose ($50\ \text{mg/kg}$) in $6\ \text{ml/kg}$ saline. An open cranial window was prepared ($2.5 \times 4.5\ \text{mm}$) using a saline-cooled drill to access the neocortex of the right hemisphere (posterior $3.3\ \text{mm}$ to anterior $1.2\ \text{mm}$ from bregma). The dura was removed and great care was taken to avoid triggering premature

SDs. ACSF was topically applied to the brain containing in mmol/L: $127.5\ \text{NaCl}$, $24.5\ \text{NaHCO}_3$, $6.7\ \text{urea}$, $3.7\ \text{glucose}$, $3\ \text{KCl}$, $1.5\ \text{CaCl}_2$, and $1.2\ \text{MgCl}_2$. The ACSF was equilibrated with a gas mixture containing 6.6% O_2 , 5.9% CO_2 , and 87.5% N_2 . A second small (diameter $\sim 1\ \text{mm}$, posterior $3.6\ \text{mm}$, lateral $2.0\ \text{mm}$ from bregma) burr hole allowed for stimulation of the cortex through the intact dura mater. Regional cerebral blood flow (rCBF) was continuously monitored with one laser-Doppler flow (LDF) probe (Periflux 4001, Perimed, Järfälla, Sweden). The subdural direct current-electrocorticography (DC-ECOG) (bandpass: $0\text{--}45\ \text{Hz}$) was recorded using an Ag/AgCl microelectrode. Changes in the extracellular K^+ concentration ($[\text{K}^+]_o$) and the intracortical DC shift (bandpass $0\text{--}45\ \text{Hz}$) were recorded in a cortical depth of $150\ \mu\text{m}$ using two ISMEs, positioned at the opposing ends of the window. A reference electrode (Ag/AgCl pellet) was placed subcutaneously above the nose. Body temperature was maintained at 37°C using a heating pad (Temperature Control FHC, Bowdoinham, ME, USA). The level of anesthesia was assessed by monitoring breathing rate and testing motor responses to foot-pinching. Electrical stimuli of increasing intensity were applied using a bipolar stimulation electrode (tip diameter: $0.2\ \text{mm}$, tip separation: $0.5\ \text{mm}$, model: NE-200, Rhodes Medical Instruments, Summerland, CA, USA) connected to a battery-driven stimulus isolator (BSI-1, BAK Electronics). The stimulation protocol consisted of biphasic pulses of $100\ \text{ms}$ ($\pm 50\ \text{ms}$) duration with exponentially increasing intensities ($20, 30, 40, 50, 60, 80, 100, 150, 200, 260, 340, 450, 600, 800, 1000\ \mu\text{A}$) at 5-min intervals until SD was triggered.³³ SD threshold was defined as the smallest electrical charge (electric current [A] \times time [s]) necessary to trigger an SD. Analog-to-digital conversion was performed using a Power 1401 (Cambridge Electronic Design). $[\text{K}^+]_o$, voltage and rCBF changes were continuously recorded using a personal computer and Spike2 software (version 6, Cambridge Electronic Design). Animals were killed after the experiment by intravenous administration of KCl solution. SD speed was calculated by dividing the distance between the ISME tips by the latency between SD onset as recorded by the occipital and rostral electrode.

Data analysis, visualization and statistical inference

Unless not stated otherwise, all data are given as mean \pm standard deviation. Boxplots show the median and interquartile range (IQR). The whiskers extend to the most extreme data point that is no more than 1.5 times IQR from the edge of the box. More extreme data points (outliers) are shown as gray plus signs. In addition, the arithmetic mean is included as a red

triangle. For clarity, time-series data or related data points with error bars are given as mean \pm standard error of the mean (SEM). If desired, standard deviation can be calculated as SEM*sqrt(n) using the sample size given in the text. Assessment of data distribution and statistical testing was performed using the scientific Python stack³⁴ and graphs were prepared using Matplotlib.³⁵

Supplementary materials and methods

Further information on data analysis and statistical inference, K⁺-sensitive microelectrodes, [K⁺]_o threshold for SD induction, stimulus-induced [K⁺]_o increases, KCl microinjection SD threshold, intrinsic optical signal (IOS) recordings, in-vivo experiments under isoflurane anesthesia, and Na⁺/K⁺-ATPase activity assay.

Results

Deficiency of the $\alpha 2$ isoform increases SD susceptibility in acute brain slices when exposed to high [K⁺]_o in the bathing medium

To obtain a measure of SD susceptibility in acute brain slices, we raised [K⁺]_o in a stepwise fashion in 30-min intervals until SD occurred (Figure 1(a) to (c)). In most slices, SDs originated in the neocortex and, in contrast to physiological [K⁺]_o, SDs were not confined to the cortex but frequently invaded the hippocampus in coronal or the striatum in transverse brain slices (Figure 1(a)). In slices from $\alpha 2^{+/KOE4}$ mice, SD was initiated at a significantly lower [K⁺]_o (13.0 \pm 1.2 mmol/L, $n=18$) compared to their wild-type littermates (WT) (14.9 \pm 1.7 mmol/L, $n=23$; $P=0.001$) (Figure 1(d)). The SD threshold reduction was reflected in a significant shortening of the latency to SD occurrence ($\alpha 2^{+/KOE4}$: 62.1 \pm 16.0 min, $n=18$; WT: 79.9 \pm 21.6 min, $n=23$; $P=0.004$) (Figure 1(e)). These results indicate that $\alpha 2$ haploinsufficiency results in increased SD susceptibility under elevated baseline [K⁺]_o. In contrast to the threshold effect, peak [K⁺]_o and [K⁺]_o undershoot were not significantly affected by $\alpha 2$ deficiency (Figure 1(f) and (g)).

To compare the magnitude of the observed SD effects of genetic $\alpha 2$ isoform reduction with the effect of pharmacological Na⁺/K⁺-ATPase inhibition, we co-applied 5 μ mol/L ouabain with the high [K⁺]_o bathing medium of WT brain slices. In this concentration, ouabain blocks most of the $\alpha 2/3$ portion of the Na⁺/K⁺-ATPase activity.^{5,36} The pharmacological effect on SD latency ($\alpha 2^{+/KOE4}$: -22.2%, ouabain: -22.6%) and SD threshold reduction was of similar magnitude compared to genetic $\alpha 2$ isoform reduction observed in $\alpha 2^{+/KOE4}$ mice ($\alpha 2^{+/KOE4}$: -12.7%, ouabain: -16.4%).

To investigate the contribution of the astrocytic ($\alpha 2$) and the neuronal ($\alpha 3$) isoform to the effect of ouabain inhibition, we added 5 μ mol/L ouabain to the high [K⁺]_o of brain slices from $\alpha 2$ -deficient mice. Although adding ouabain to the bathing medium of $\alpha 2^{+/KOE4}$ brain slices further lowered (4.7%) the threshold [K⁺]_o and further reduced the SD latency by 12.7% in $\alpha 2^{+/KOE4}$ compared to WT, these effects were considerably smaller compared to the effect of ouabain in WT slices and did not reach statistical significance (Figure 1(d) and (e)). These results suggest that the facilitating effect of ouabain on SD is mediated via the astrocytic isoform. If the neuronal isoform would be involved, the ouabain effect would be expected to add significantly to the effect of genetic $\alpha 2$ reduction in $\alpha 2^{+/KOE4}$ mice. Instead, the size of the ouabain effect was reduced in $\alpha 2$ -deficient mice, which is consistent with the reduced ouabain receptor availability. Interestingly, only pharmacological Na⁺/K⁺-ATPase inhibition using 5 μ mol/L ouabain significantly prolonged SD duration and reduced DC amplitude, whereas genetic $\alpha 2$ reduction did not have these effects (Figure 1(h) and (i)).

Despite the effect of genetic $\alpha 2$ reduction on SD threshold and latency, SD speed was similar in $\alpha 2^{+/KOE4}$ mice compared to WT ($\alpha 2^{+/KOE4}$: 9.2 \pm 2.0 mm/min, $n=16$; WT: 8.8 \pm 1.5 mm/min, $n=21$; $P=0.29$) under high [K⁺]_o (Figure 1(j)). Because [K⁺]_o elevation exerts a strong effect on SD speed (high [K⁺]_o: 317% of control in 3 mM [K⁺]_o), a significant speed difference is presumably negated by the lower threshold [K⁺]_o in $\alpha 2^{+/KOE4}$ mice; 5 μ M ouabain did not have a facilitating effect on SD speed under high [K⁺]_o either (ouabain: 8.3 \pm 1.1, $n=21$; control: 8.8 \pm 1.5, $n=21$, $P=0.34$).

Deficiency of other Na⁺/K⁺-ATPase α isoforms does not affect SD susceptibility under elevated baseline [K⁺]_o in brain slices

Next, we sought to determine whether the observed SD threshold [K⁺]_o effect in $\alpha 2^{+/KOE4}$ mice was specific to a genetic reduction of this particular isoform or whether the effect could be mimicked by deficiency of the other Na⁺/K⁺-ATPase isoforms expressed in the brain: $\alpha 1$ and $\alpha 3$. To this end, we tested the high [K⁺]_o protocol with $\alpha 1^{+/KOE15}$ and $\alpha 3^{+/KOE14}$ mice and compared the results to their wild-type littermates (WT).

Whereas lower [K⁺]_o triggered SD in $\alpha 2^{+/KOE4}$ mice, we did not find a significant difference between the threshold [K⁺]_o in $\alpha 3^{+/KOE14}$ (103.7 \pm 14.3% of WT, $n_{het}=13$, $n_{WT}=14$; $P=0.5$) or $\alpha 1^{+/KOE15}$ (94.2 \pm 9.9% of WT, $n_{het}=6$, $n_{WT}=8$; $P=0.48$) compared to WT (Figure 2(a)). These observations were confirmed by the absence of differences in latency to SD initiation

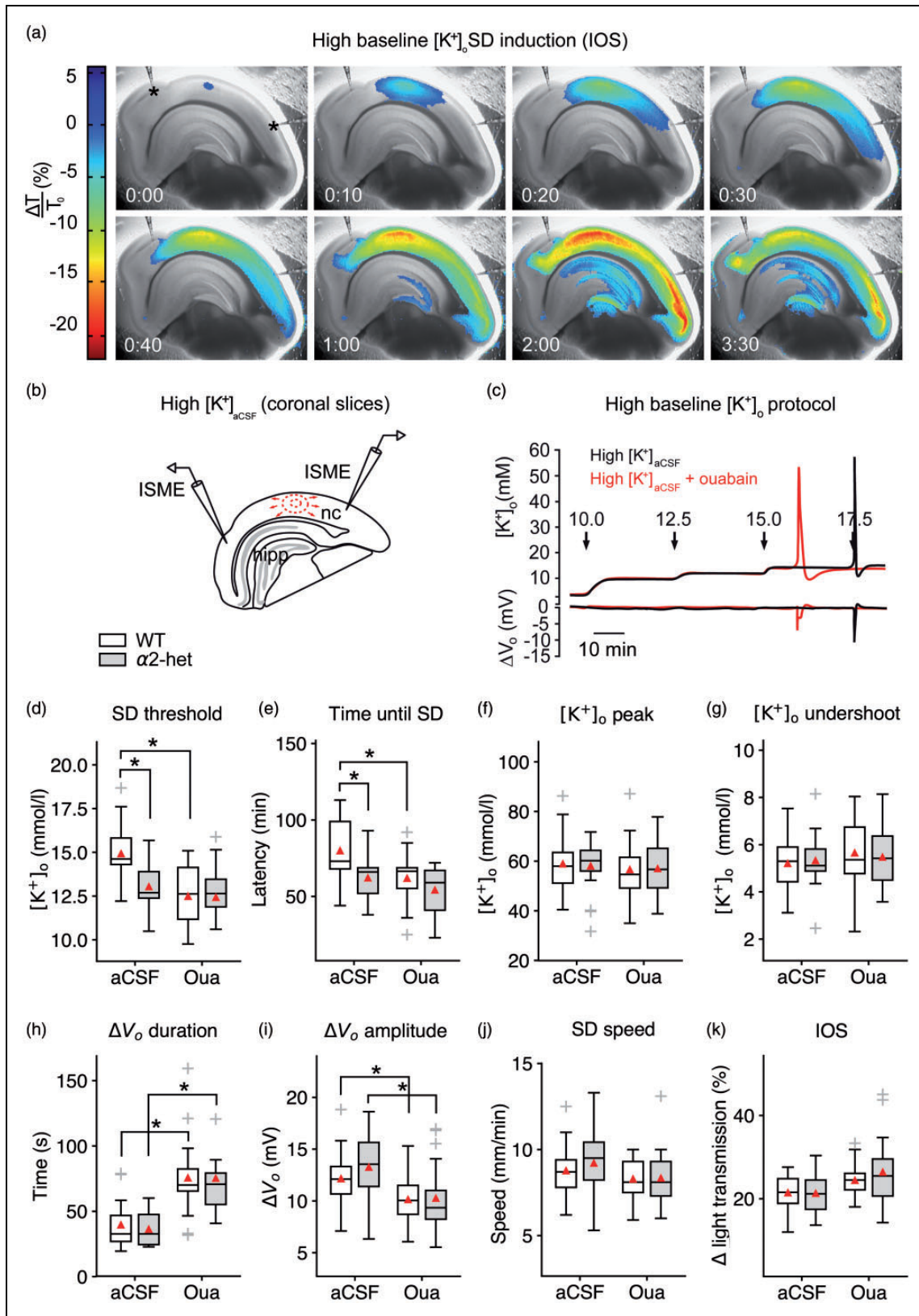


Figure 1. Na^+/K^+ -ATPase $\alpha 2$ deficiency increases SD susceptibility in acute brain slices. (a–b) SD speed and invaded area were imaged using light transmission changes (IOS). In the interface-type recording chamber, SD is characterized by a short increase (blue), followed by a long-lasting decrease of the IOS (red). Elevated baseline $[K^+]_o$ induced SD in the neocortex (nc) and frequently in the

(continued)

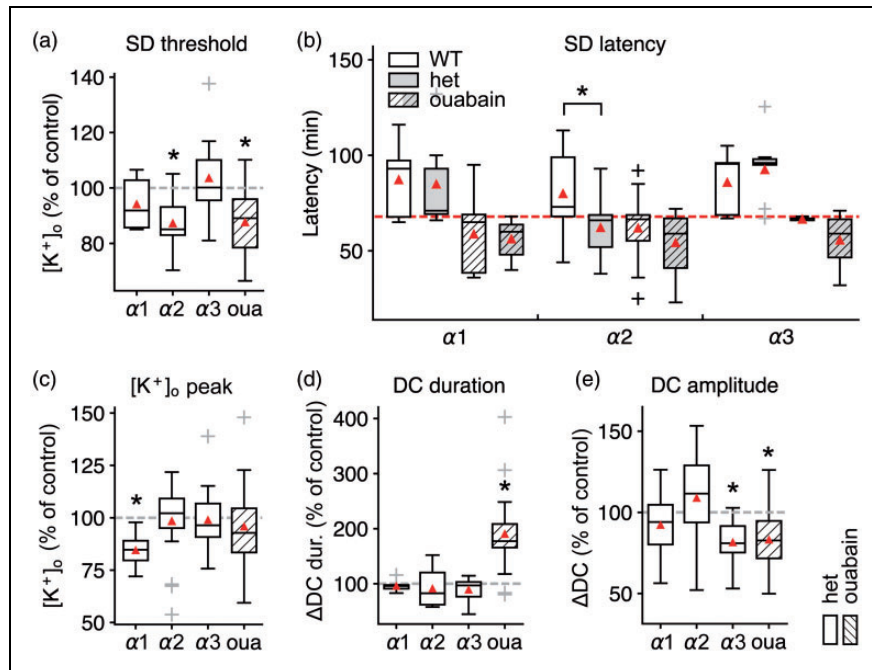


Figure 2. SD threshold reduction is specific to deficiency of the $\alpha 2$ isoform in acute brain slices. (a) Only $\alpha 2$ deficiency or pharmacological inhibition with 5 μM ouabain significantly reduced SD threshold $[\text{K}^+]_o$, whereas $\alpha 1$ and $\alpha 3$ deficiency did not significantly affect threshold $[\text{K}^+]_o$ as measured by ISMEs. (b) SD latency: $\alpha 2^{+/KOE4}$ segregate from the high into the low threshold group together with ouabain, indicated by the significantly shorter time until SD occurrence (below the red dashed line). (c) Peak $[\text{K}^+]_o$ during SD was significantly lower in $\alpha 1^{+/KOE15}$ mice. (d) The duration of the accompanying DC shift was longer only under ouabain exposure, whereas α isoform deficiency had no effect. (e) The DC amplitude was reduced in $\alpha 3^{+/KOE4}$ and in presence of 5 μM ouabain. Sample sizes: $\alpha 2^{+/KOE4}/\alpha 2^{+/+}$, $n = 17\text{--}23$; $\alpha 3^{+/KOE4}/\alpha 3^{+/+}$, $n = 10\text{--}14$; $\alpha 1^{+/KOE15}/\alpha 1^{+/+}$, $n = 6\text{--}8$. * $P < 0.05$.

in $\alpha 3^{+/KOE4}$ and $\alpha 1^{+/KOE15}$ compared to WT (Figure 2(b)). These results indicate that the observed SD facilitation under high $[\text{K}^+]_o$ is specific for a reduction of the $\alpha 2$ isoform and suggest that the effect is not primarily dependent on bulk Na^+ and K^+ transport capacity.

Extracellular K^+ clearance during intense neuronal stimulation is not altered significantly in $\alpha 2^{+/KOE4}$ mice

Because of the effect of $\alpha 2$ deficiency on the SD threshold in conditions of high $[\text{K}^+]_o$ challenge, we wanted to test whether impaired extracellular K^+ clearance was causal to the observed threshold differences. To this end, we analyzed stimulus-induced $[\text{K}^+]_o$ surges during and following intense neuronal stimulation in

acute brain slices (Figure 3(a) to (c)). Stimulus trains of increasing intensity lasting 10 s, consisting of 200 pulses at a frequency of 20 Hz, were applied to the Schaffer collateral pathway in the hippocampal CA1 subfield of transverse brain slices (Figure 3(a)) of $\alpha 2^{+/KOE4}$ and WT. Of note, even under supramaximal stimulation (150%), in none of the $\alpha 2^{+/KOE4}$ slices SD was triggered.

During neuronal activation, K^+ is released into the extracellular space. The $[\text{K}^+]_o$ undershoot following neuronal stimulation is believed to be predominantly attributable to Na^+/K^+ -ATPase activity, stimulated by elevated intracellular sodium concentration ($[\text{Na}^+]_i$) following intense neuronal firing. Because faster K^+ clearance mechanisms, such as passive diffusion and spatial buffering, have redistributed K^+ away

Figure 1. Continued

hippocampus (hipp) but not in the brainstem. (c) Stepwise increased baseline $[\text{K}^+]_o$ allowed for threshold assessment using ISMEs. (d) SD occurred at lower $[\text{K}^+]_{\text{ACSF}}$ in $\alpha 2^{+/KOE4}$ compared to WT. Co-application of 5 μM ouabain did not significantly add to the $\alpha 2$ deficiency effect on threshold $[\text{K}^+]_{\text{ACSF}}$ indicating ouabain action via the astrocytic and not the neuronal isoform. (e) SD latency was shorter in $\alpha 2^{+/KOE4}$ compared to WT mice confirming the lower $[\text{K}^+]_o$ threshold in $\alpha 2$ -deficient mice. (f–g) Genetic $\alpha 2$ reduction did not affect $[\text{K}^+]_o$ peak and $[\text{K}^+]_o$ undershoot following SD. (h–i) Only pharmacological inhibition of the $\alpha 2/3$ portion of the Na^+/K^+ -ATPase prolonged SD duration and decreased the DC amplitude irrespective of the genetic background. (j) SD speed was high under elevated $[\text{K}^+]_{\text{ACSF}}$ without additional effects of genetic or pharmacological $\alpha 2$ reduction. (k) IOS amplitude was not affected significantly by genetic or pharmacological $\alpha 2$ reduction. Sample sizes: $\alpha 2^{+/KOE4}$, $n = 16\text{--}19$; $\alpha 2^{+/+}$, $n = 21\text{--}23$. * $p < 0.05$.

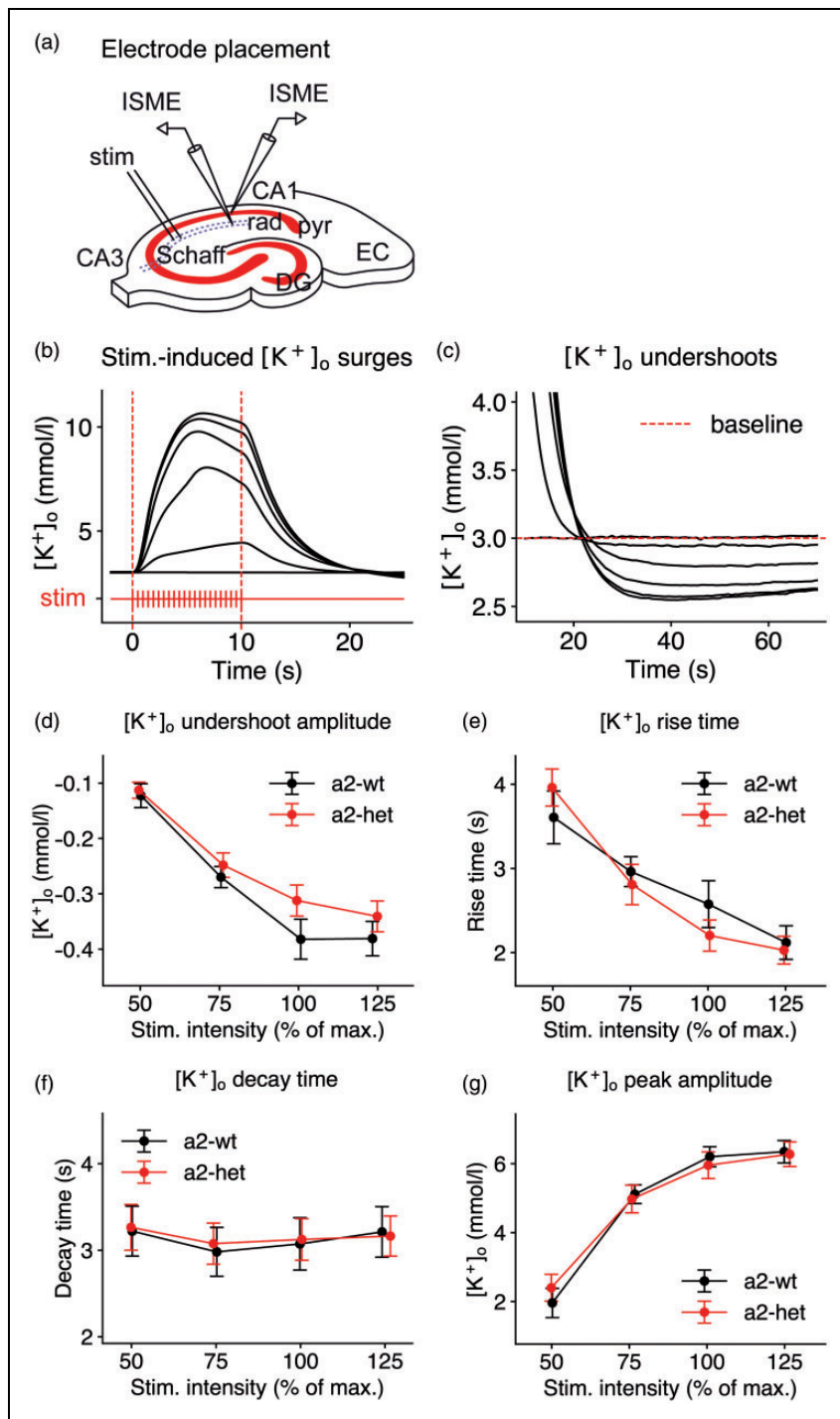


Figure 3. $[K^+]_o$ clearance is not significantly impaired in $\alpha 2$ -deficient mice. (a) A stimulus train (10 s, 20 Hz) was applied to the hippocampal Schaffer collateral pathway (Schaff) in the CA3 of transverse brain slices. stim: bipolar stimulation electrode location; rad: stratum radiatum; pyr: stratum pyramidale; EC: entorhinal cortex; DG: dentate gyrus. (b) $[K^+]_o$ surges and (c) $[K^+]_o$ undershoots were recorded in str. pyramidale and radiatum in CA1 using ISMEs. (d) The $[K^+]_o$ undershoot amplitude showed a tendency to be less pronounced at 100% stimulation intensity although the difference did not reach statistical significance ($\alpha 2^{+/KOE4}$: -0.31 ± 0.03 , $n = 19$; WT: -0.38 ± 0.04 , $n = 13$; $P = 0.13$). (e-g) $\alpha 2$ deficiency did not significantly alter the $[K^+]_o$ response to intense neuronal stimulation. Data are presented as mean \pm SEM.

from the location of its release, $[K^+]_o$ is decreasing from its baseline level and forms a noticeable undershoot.³⁷ The $[K^+]_o$ undershoot amplitude increased with higher stimulation strength and at 100% stimulation intensity, the amplitude appeared to be slightly lower in $\alpha 2^{+/KOE4}$ animals compared to WT, although the difference did not reach statistical significance (Figure 3(d)).

To test whether the $\alpha 2$ isoform is involved in limiting local K^+ accumulation in response to neuronal stimulation, we analyzed $[K^+]_o$ rise time and peak $[K^+]_o$. To assess extracellular K^+ clearance, we analyzed the $[K^+]_o$ decay time.^{25,38} We did not find significant differences in $[K^+]_o$ rise time, decay time, and peak $[K^+]_o$ amplitude between $\alpha 2^{+/KOE4}$ and WT (Figure 3(e) to (g)). The lack of an effect in acute brain slices corresponds to similar activity of Na^+/K^+ -ATPase $\alpha 2/3$ fraction measured in brain homogenates of $\alpha 2$ and WT (Supplementary Figure 1 and Table 1).

The data indicate that the extracellular K^+ clearance during intense neuronal stimulation is not significantly compromised in $\alpha 2^{+/KOE4}$ mice in normal ACSF. This observation is in agreement with data from $\alpha 2^{+/G301R}$ mice in a similar protocol³⁹ but contrasts with the findings in slices of $\alpha 2^{+/W887R}$ mice, that displayed a higher time constant of the $[K^+]_o$ decay following the stimulation train compared to WT.²⁵

In contrast to high $[K^+]_o$, SD threshold and speed are not affected in $\alpha 2^{+/KOE4}$ mice under physiological $[K^+]_o$

Published FHM mouse models exhibit a high SD susceptibility phenotype characterized by a low SD threshold and increased SD speed^{25,33,40} as well facilitated corticostriatal SD propagation.²⁷

To assess the SD threshold without globally affecting $[K^+]_o$, we injected increasing amounts of KCl (1M) focally into the cortical tissue until SD was triggered under normal $[K^+]_o$ (3 mM) (Figure 4(a) and (b)). In contrast to the higher SD susceptibility under elevated baseline $[K^+]_{ACSF}$, the focal induction duration and thus the injected K^+ volume were similar in $\alpha 2^{+/KOE4}$ mice compared to WT under physiological $[K^+]_o$ (Figure 4(c)). We calculated the SD speed using the SD-associated light transmittance (LT) changes (IOS) in the dorsal and the ventral portion of the propagation path (Figure 4(d)). Although we found significantly higher SD speed in the dorsal compared to ventral portion of the cortex (dorsal: 3.2 ± 0.7 , $n=9$; ventral: 2.4 ± 0.4 , $n=9$; $P=0.01$) (Figure 4(e)), SD speed was not different between $\alpha 2^{+/KOE4}$ and WT ($\alpha 2^{+/KOE4}$: 2.6 ± 0.5 mm/min, $n=9$; WT: 2.8 ± 0.5 mm/min; $P=0.86$) (Figure 4(f)). We also analyzed the extent of SD spread as the projected area of the IOS change on the brain slice surface and did not find an effect of $\alpha 2$

deficiency ($\alpha 2^{+/KOE4}$: 3.3 ± 1.3 mm², $n=10$; WT: 3.9 ± 1.3 mm²; $P=0.38$) (Figure 4(g)). Whereas α isoform deficiency in general did not have an effect on SD speed and extent of SD spread, 5 μ M ouabain increased SD speed significantly and resulted in larger extent of SD spread in brain slices (Figure 4(g) and (h)).

The data indicate that $\alpha 2$ deficiency is well compensated under normal $[K^+]_o$, in contrast to prolonged exposure to elevated baseline $[K^+]_o$. The observation of similar SD susceptibility under normal $[K^+]_o$ is unexpected and differs from studies using brain slices of FHM1⁴⁰ and FHM2²⁵ knock-in mice. Both studies reported a lower SD threshold and higher SD speed albeit using a submerged system and not an interface recording chamber as employed in this study. However, the absence of an effect on SD speed has been reported in another study comparing FHM2 knock-in mice ($\alpha 2^{+/G301R}$) with WT in-vivo,²⁴ indicating possible functional differences between distinct FHM2 missense mutations. Despite the aforementioned differences in the recording chamber setup, we expect the brain slice speed measurement approach to be sensitive enough to detect the reported speed differences, since application of 5 μ M ouabain resulted in a massive speed increase (Figure 4(h)). Furthermore, the measurement uncovered a significant difference between the dorsal and the ventral portion of the mouse cortex which was consistent throughout all mouse lines. Additionally, the dorso-ventral SD speed gradient was also evident as a section-dependence of SD speed in transverse slices (data not shown).

SD susceptibility in-vivo

To test the SD threshold in-vivo, we induced SD electrically in the right hemisphere of urethane/ α -chloralose anesthetized Na^+/K^+ -ATPase α isoform-deficient mice. Biphasic stimuli of increasing strength were applied through a bipolar stimulation electrode until SD was recorded by an intracortical microelectrode in the open cranial window (Figure 5(a)). Because of a possible impact on the SD threshold and a drastically different rCBF response of a secondary SD,⁴¹ we assessed the typical multiphasic rCBF response of the mouse using LDF (Figure 5(b)). To test SD susceptibility under different anesthesia and to precisely check for potential induction of premature SDs during the preparation phase, we induced SDs electrically in animals anesthetized with isoflurane in a second set of experiments. LASCA imaging was employed to map cerebral perfusion levels through the intact skull bone of both hemispheres (Figure 5(c) and (d), Supplementary Figure 2).

Confirming the brain slice experiments in normal ACSF of this study, $\alpha 2$ -deficient mice did not display a reduction in the threshold electric charge to induce

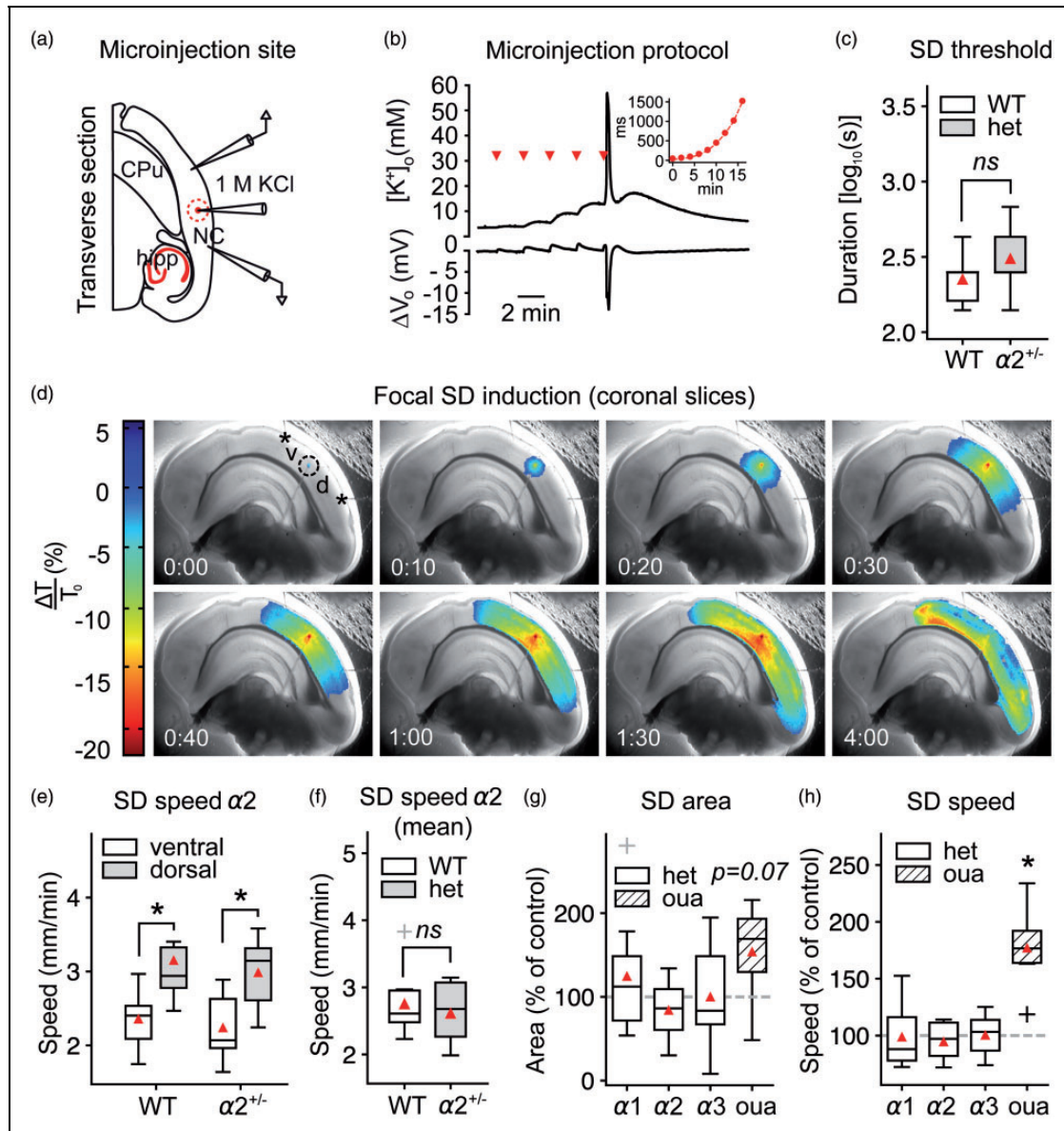


Figure 4. SD speed is not affected by $\alpha 2$ -deficiency in acute brain slices. (a–b) SD was induced focally in acute coronal brain slices under physiological ACSF by microinjecting an increasing volume of 1M KCl into the tissue. NC: neocortex; hipp: hippocampus; CPU: caudate putamen (c) The necessary injected 1M KCl volume to evoke SD was similar in $\alpha 2^{+/KOE4}$ and $\alpha 2^{+/+}$ mice under normal $[K^+]_{ACSF}$ ($\alpha 2^{+/KOE4}$: $n = 9$, $\alpha 2^{+/+}$: $n = 6$). (d) SD speed and area were calculated from the dorsal (“d”) and ventral (“v”) portion relative to injection point (dashed circle) in coronal brain slices. (e) SD propagated with markedly higher speed in the dorsal compared to the ventral portion of the cortex as measured from the injection site. (f) SD speed was not different between $\alpha 2^{+/KOE4}$ and WT (mean of dorsal and ventral speeds) under normal $[K^+]_{ACSF}$. Data were obtained from 9 $\alpha 2^{+/KOE4}$ (39 SDs, 27 slices) and 9 $\alpha 2^{+/+}$ (37 SDs, 25 slices) mice. (g) The projected area of SD spread on the slice surface tended to be larger ($P = 0.07$) only in ouabain-treated slices with no effect in $\alpha 2^{+/KOE4}$ mice. (h) Ouabain application increased SD speed drastically ($77.3 \pm 35.2\%$, $P < 0.00001$), whereas genetic α isoform deficiency had no effect on SD speed. Sample sizes for speed and area calculations: $\alpha 2^{+/KOE4}/\alpha 2^{+/+}$, $n = 9$; $\alpha 3^{+/KOE14}/\alpha 3^{+/+}$, $n = 9$ –16; $\alpha 1^{+/KOE15}/\alpha 1^{+/+}$, $n = 8$; ouabain, $n = 7$. * $P < 0.05$.

SD in-vivo. In fact, the threshold charge tended towards higher threshold charges in $\alpha 2^{+/KOE4}$ mice, although the difference did not reach statistical significance ($\alpha 2^{+/KOE4}$: $58.1 \pm 38.5 \mu C$, $n = 10$, WT: $33.4 \pm 24.3 \mu C$, $n = 12$, $P = 0.15$) (Figure 5(e)). In mice deficient

of the $\alpha 3$ isoform, the SD threshold charge was significantly higher compared to WT ($\alpha 3^{+/KOE14}$: $51.8 \pm 28.3 \mu C$, $n = 9$, WT: $24.0 \pm 14.9 \mu C$, $n = 11$, $P = 0.04$). No effect of α isoform deficiency on SD threshold was observed in $\alpha 1^{+/KOE15}$ compared to WT ($\alpha 1^{+/KOE15}$: $26.5 \pm 16.7 \mu C$,

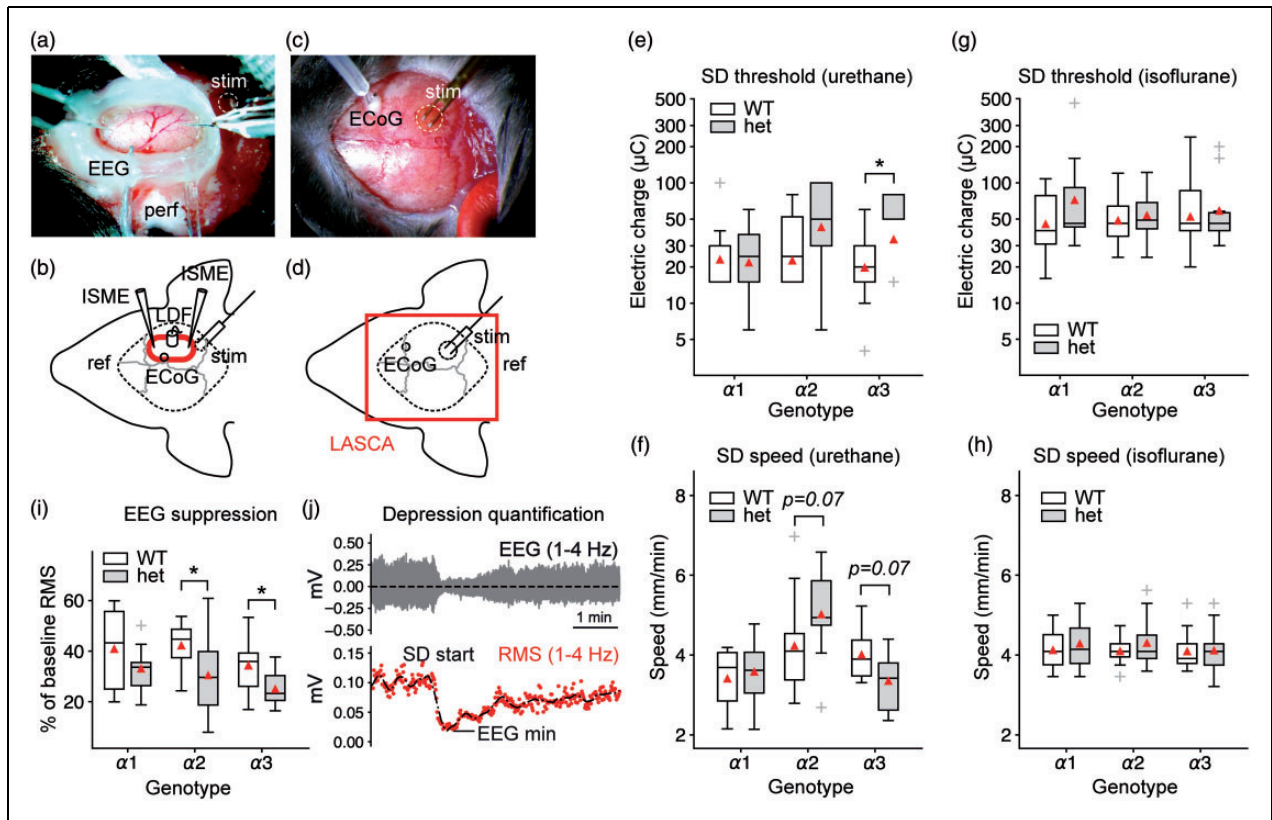


Figure 5. Na^+/K^+ -ATPase α isoform deficiency and anesthesia differentially affect SD threshold and speed. (a–b) Urethane/ α -chloralose protocol with open cranial window preparation and experimental setting. LDF: laser Doppler flowmetry probe; LASCA: laser speckle contrast analysis imaging area; ref: reference electrode; ECoG: electrocorticography electrode; perf: ACSF perfusion; stim: site of electrical stimulation; ECoG: epidurally placed electrode (c–d) Isoflurane protocol with LASCA imaging through the intact mouse skull. (e) In agreement with acute brain slice experiments under normal $[\text{K}^+]_o$, $\alpha 2^{+/KOE4}$ mice do not display a lower SD threshold. Mice deficient for the $\alpha 3$ isoform required a higher threshold charge to trigger SD. Y-axis shows electric charge in micro Coulomb of logarithmically transformed data. (f) In $\alpha 2^{+/KOE4}$ mice, SD speed showed a tendency towards higher values, whereas the speed tended to be lower in $\alpha 3^{+/KOE4}$ animals. Both observations did not reach statistical significance. (g–h) α isoform deficiency had no effect on SD threshold and speed under isoflurane anesthesia. (i) Depression of spontaneous activity following SD was more pronounced in heterozygous knock-out mice of all lines ($\alpha 1$, $\alpha 2$, $\alpha 3$) compared to their wild-type littermates. Differences reached statistical significance ($P < 0.05$) in $\alpha 2$ -het and $\alpha 3$ -het animals ($\alpha 2$: $P = 0.04$, $\alpha 3$: $P = 0.03$). (j) Example of spontaneous activity depression with subsequent recovery. EEG suppression was calculated as RMS amplitude reduction of the bandpass-filtered (1–4 Hz). RMS: root mean square. V_o : extracellularly recorded voltage.

$n = 10$, WT: $29.0 \pm 26.5 \mu\text{C}$, $n = 10$, $P = 0.91$). SD speed trended towards higher values in $\alpha 2$ -deficient mice, although this difference did not reach statistical significance at the 5% level ($\alpha 2^{+/KOE4}$: $5.0 \pm 1.2 \text{ mm/min}$, $n = 9$; WT: $4.2 \pm 1.2 \text{ mm/min}$, $n = 13$; $P = 0.07$) (Figure 5(f)). In contrast to $\alpha 2$ -deficient mice, $\alpha 3^{+/KOE4}$ mice displayed a lower SD speed, although the difference did not reach statistical significance ($\alpha 3^{+/KOE4}$: 3.4 ± 0.8 , $n = 9$; WT: 4.0 ± 0.7 , $n = 8$; $P = 0.07$). Changes in DC and $[\text{K}^+]_o$ during SD did not differ significantly between α isoform deficient mice and WT (Supplementary Figure 3). No significant differences were observed in SD threshold and speed comparing $\alpha 1^{+/KOE15}$, $\alpha 2^{+/KOE4}$, and $\alpha 3^{+/KOE4}$ to WT when using isoflurane anesthesia (Figure 5(g) and (h)).

ECoG depression following SD is pronounced in $\alpha 2$ - and $\alpha 3$ -deficient mice

In electrically active tissue, SD causes spreading depression of spontaneous neuronal activity. To compare ECoG depression between α isoform-deficient mice and WT, we calculated the initial reduction of the root mean square (RMS) amplitude of the bandpass-filtered (1–4 Hz) ECoG following SD. The ECoG depression was more pronounced in $\alpha 2$ isoform-deficient mice ($\alpha 2^{+/KOE4}$: $30.4 \pm 15.5\%$, $n = 10$; WT: $42.2 \pm 10.0\%$, $n = 9$; $P = 0.045$) and $\alpha 3^{+/KOE4}$ mice ($\alpha 3^{+/KOE4}$: $25.0 \pm 7.4\%$, $n = 8$; WT: $34.3 \pm 10.7\%$, $n = 13$; $P = 0.033$) compared to WT. ECoG suppression was not significantly different in $\alpha 1^{+/KOE15}$ compared to WT ($P = 0.4$) (Figure 5(i) and (j)).

The result of a pronounced initial reduction of spontaneous activity with largely normal recovery in $\alpha 2$ -deficient mice is in agreement with data from another $\alpha 2$ knock-out mouse model.⁴² In this study, only $\alpha 2^{+/KOE2}$ mice displayed a difference in the ECoG suppression, whereas the effect was not observed in $\alpha 2^{KOE21}$ mice⁴² indicating different degrees of functional impairment following N- and C-terminal deletions in the knock-out mice. A slowed recovery of the spreading depression as assessed by the spontaneous activity in the ECoG has also been reported in a knock-in mouse model of FHM2,²⁴ whereas evoked potentials recovered in a similar fashion to wild-type animals in the same study and in two FHM1 mouse models.²⁷

Pronounced post SD oligemia in $\alpha 2$ -deficient mice under urethane/ α -chloralose anesthesia

Under physiological conditions, the cerebral hemodynamic response to SD is characterized by a considerable hyperemia followed by a post-SD oligemia in most species, such as humans and rats.⁴³ The rCBF response in mice differs drastically from other studied species⁴¹ (Figure 6(a)). Typical for the vasomotor response in mice is a pronounced fast initial hypoperfusion that is temporally correlated with the DC shift, a short-lasting rCBF recovery, followed by a pronounced oligemic phase that can last up to an hour (Figure 6(b) to (d), Supplementary Figure 4).

rCBF was measured using an LDF probe centered between two ISMEs in the open cranial window of α isoform deficient mice and WT. In $\alpha 2$ -deficient mice, the hypoemic response to SD was significantly more pronounced compared to WT. Both the initial short hypoperfusion ($\alpha 2^{+/KOE4}$: $44.3 \pm 13.9\%$, $n = 10$; $\alpha 2^{+/-}$: $66.8 \pm 21.3\%$, $n = 11$; $p = 0.01$) and the long-lasting hypoemia, as measured 10 min after the short, transient recovery ($\alpha 2^{+/KOE4}$: $53.5 \pm 20.1\%$, $n = 9$; $\alpha 2^{+/-}$: $78.4 \pm 19.1\%$, $n = 11$; $p = 0.009$), decreased by over 30% in $\alpha 2^{+/KOE4}$ mice compared to WT (Figure 6(e) and (f)). No significant differences in the post SD perfusion were apparent in $\alpha 3^{+/KOE14}$ and $\alpha 1^{+/KOE15}$ compared to WT. The pronounced hypoemia in $\alpha 2^{+/KOE4}$ mice suggests a specific role of the $\alpha 2$ isoform in regulation of the diameter of cerebral vasculature.

Discussion

Increased SD susceptibility in brain slices is specific for $\alpha 2$ haploinsufficiency

In this study, we show that the genetic reduction of the three different Na^+/K^+ -ATPase α isoforms expressed in the mammalian brain results in distinct SD phenotypes. Only $\alpha 2^{+/KOE4}$ mice displayed a lower SD threshold in

acute brain slices. In principle, this result is in agreement with studies in FHM2 mouse models and supports evidence that $\alpha 2$ haploinsufficiency results in increased SD susceptibility.^{23–25} However, the threshold effect in $\alpha 2^{+/KOE4}$ mice was only present in acute brain slices when the tissue was exposed to elevated baseline $[\text{K}^+]_o$ for an extended period of time. Under normal conditions, the SD threshold was similar to WT in acute brain slices and in-vivo. These findings present a notable difference in the SD phenotype when compared to data from one of the two published FHM2 knock-in mouse lines ($\alpha 2^{+/W887R}$)^{23,25} and a recent knock-out mouse study,⁴² where an effect on SD threshold was demonstrated under normal $[\text{K}^+]_o$.

Moreover, in normal ACSF, extracellular K^+ clearance during and following intense neuronal stimulation was not significantly compromised in $\alpha 2^{+/KOE4}$ mice. Although this observation is consistent with data from $\alpha 2^{+/G301R}$ mice in a similar protocol,³⁹ it contrasts with the findings in slices of $\alpha 2^{+/W887R}$ mice, that displayed a higher time constant of the $[\text{K}^+]_o$ decay following the stimulation train compared to WT.²⁵

The in-vivo recordings support the findings in acute brain slices from $\alpha 2^{+/KOE4}$ mice. Using two separate experimental paradigms with either urethane/ α -chloralose or isoflurane anesthesia, we found no reduction in the electric charge to trigger SD in $\alpha 2^{+/KOE4}$ mice compared to WT. However, although isoflurane has been employed successfully in SD studies^{44,45} including electrical SD induction,²⁸ the results have to be interpreted with caution, since isoflurane inhibits N-methyl-D-aspartate (NMDA) receptors⁴⁶ and has been reported to suppress SD.^{47–50}

The differences between the mild SD phenotype of $\alpha 2^{+/KOE4}$ mice and published FHM mouse models may be attributable to differences in the genetic modifications of the murine ATP1A2 in knock-out and knock-in mice. Whereas FHM2 mouse models bear missense mutations resulting in the substitution of only a single amino acid,^{23,24} expression of the null allele in $\alpha 2^{+/KOE4}$ mice would lead to an $\alpha 2$ isoform truncated after the first transmembrane domain that would lack approximately 90% of the original protein.¹⁴ In consequence, the protein would be deficient of essential functional elements, such as the nucleotide-binding (N), the phosphorylation (P), and the actuator (A) domain, which is expected to result in full haploinsufficiency.^{51,52}

It seems unlikely that the milder SD phenotype of $\alpha 2^{+/KOE4}$ mice is caused by compensatory overexpression of $\alpha 1$ and/or $\alpha 3$, as semi-quantification of protein and RNA expression has been demonstrated to be at normal levels for $\alpha 1$ and even showed a ~25% reduction in the $\alpha 3$ isoform.²⁶ Moreover, since $\alpha 1$ -deficiency was not associated with increased SD susceptibility and

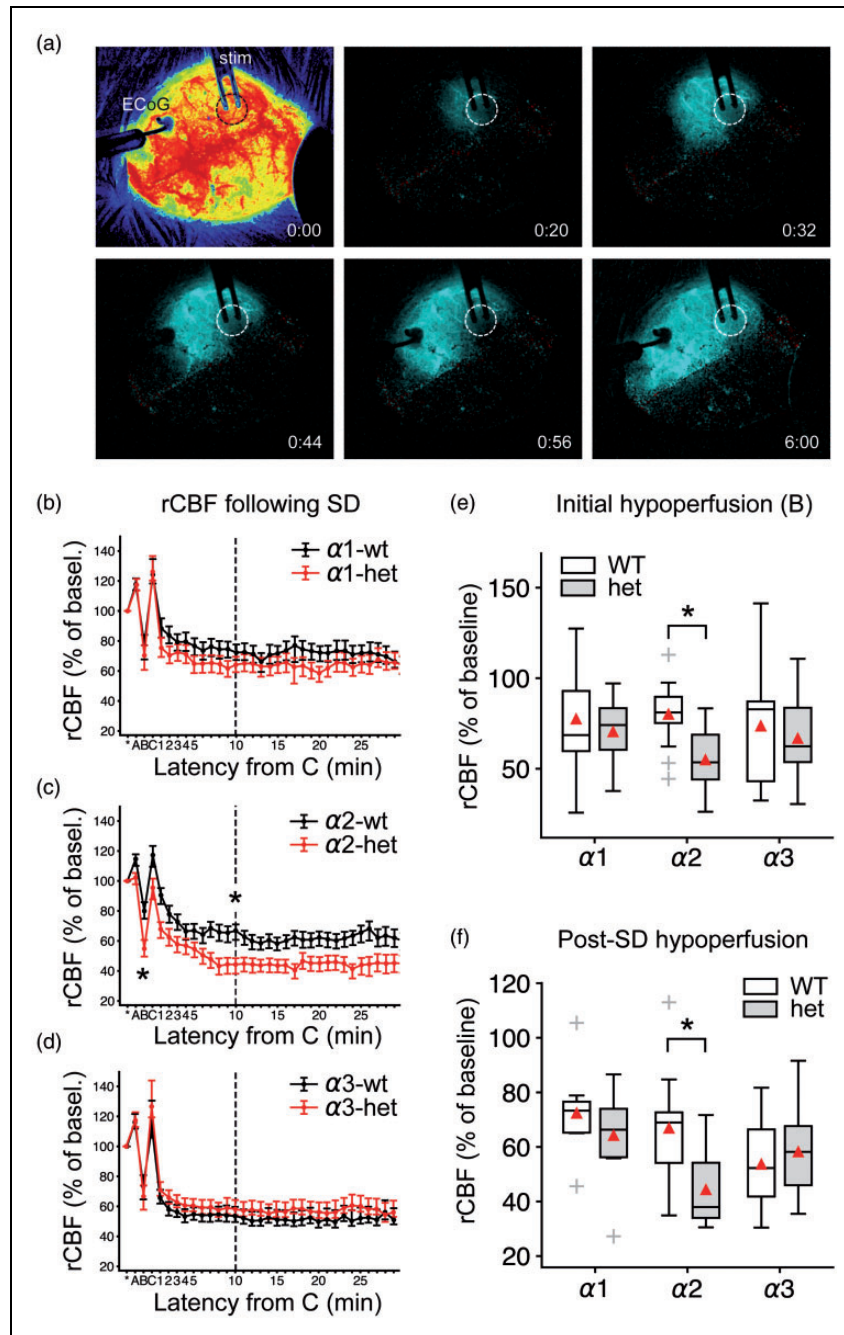


Figure 6. Pronounced hypoperfusion in $\alpha2$ -deficient mice in the wake of SD under urethane/ α -chloralose anesthesia. (a) LASCA imaging in the isoflurane protocol: The first image shows cortical perfusion imaged through the intact mouse skull. Starting from the second image, difference images show the propagating hypoperfusion that characterizes SD in the mouse cortex of the right hemisphere. Regional CBF over time was analyzed and SD speed was calculated. The dashed circle marks the burr hole with the exposed dura mater. Time from SD onset is given in [m:ss] in the lower right. ECoG: electrocorticography, stim: stimulation electrode. (b–d) SD evoked a multiphasic rCBF response in mice denoted A, B, C on the time axis. A: short hyperemia, B: short-lasting hypoemia, C: hyperemia, followed by a long-lasting hypoemia (after C). Data points are given with respect to 5-min baseline rCBF (=100%) prior to SD onset as mean \pm SEM. (e–f) In $\alpha2^{+/KOE4}$ mice, the rCBF following SD showed a pronounced hypoemia in the wake of SD compared to WT during the initial hypoperfusion (marked “B”) and during the long-lasting hypoperfusion following the short rCBF recovery (marked “C”). By contrast, deficiency of $\alpha1$ and $\alpha3$ did not affect post-SD rCBF.

$\alpha 3^{+/KOE4}$ mice were more resistant against electrical SD induction in-vivo, interpretation of a possible compensatory overexpression would not be straightforward.

Phenotypic variability can also be observed between other mouse models of Na^+/K^+ -ATPase $\alpha 2$ haploinsufficiency. For example, Uekawa et al.⁴² reported higher SD susceptibility in knock-out mice with the N-terminal deletion targeting exon 2 ($\alpha 2^{+/KOE2}$) compared to animals carrying a C-terminal deletion in exon 21 ($\alpha 2^{+/KOE21}$). Heterogeneous results have also been reported for FHM2 knock-in mice. In contrast to $\alpha 2^{+/W887R}$ mice,^{23,25} $\alpha 2^{+/G301R}$ mice displayed a similar SD speed compared to WT²⁴ and did not exhibit a significantly affected $[\text{K}^+]_o$ clearance.³⁹

It seems plausible that differences in experimental approaches contribute to the observed variability of the SD phenotype between different genetically engineered mouse models of $\alpha 2$ deficiency. For example, in this study, we encountered profound SD phenotype differences in the $\alpha 3^{+/KOE4}$ group when using two different experimental approaches in-vivo. The experimental paradigms differed primarily in anesthesia and preparation to gain access to the mouse neocortex for SD induction and recording (open cranial window and ACSF perfusion vs. small burr holes with intact dura mater). Varying anesthetic regimen and SD induction methods have been employed by the other mouse model studies referred to in this article. In the first published FHM-2 mouse model study, Leo et al.²³ used urethane to anesthetize $\alpha 2^{+/W887R}$ knock-in mice and induced SD electrically.²³ By contrast, in the other published FHM-2 mouse model ($\alpha 2^{+/G301R}$), Bottger et al.²⁴ used α -chloralose as the main anesthetic and induced SD by injecting potassium acetate into the neocortical tissue. Yet another approach was used by Uekawa et al.,⁴² who investigated SD susceptibility in two distinct $\alpha 2$ knock-out mice using urethane anesthesia and triggering SD by applying increasing concentrations of KCl solution to the brain surface.

Apart from differences in experimental conditions, the observed phenotypic variability in FHM2 mouse models may reflect the remarkably diverse functional abnormalities described as a consequence of over 80 human disease-linked FHM2 mutations.⁵²

Lack of a single allele of the $\alpha 2$ isoform gene seems to be well compensated in metabolically intact in contrast to stressed tissue

Physiological neuronal activity results in local $[\text{K}^+]_o$ transients of only 0.2–0.4 mM above baseline.^{53,54} During vigorous electrical stimulation, $[\text{K}^+]_o$ locally rises up to the so-called ceiling level of ~ 12 mM.^{54–56} During SD, $[\text{K}^+]_o$ rapidly increases to a level of ~ 50 mM.⁵⁷ In addition to astrocyte-mediated spatial

buffering,^{58–60} the $\alpha 2$ isoform is ideally suited to oppose such acute rises in $[\text{K}^+]_o$ because of its low affinity, which allows the enzyme to rapidly adapt its turnover over a large range of $[\text{K}^+]_o$.^{61,62} In parallel, $\alpha 2$ activity increases in response to the membrane depolarizing effect of rising $[\text{K}^+]_o$,^{63,64} particularly when associated with the $\beta 2$ subunit.³⁹ Further, the maximal catalytic turnover (V_{max}) of the $\alpha 2$ isoform is several fold higher than that of the $\alpha 3$ isoform for example.^{61,65,66}

The $\alpha 2$ isoform is also ideally located to counteract acute rises in extracellular glutamate which typically accompany rises in $[\text{K}^+]_o$. In adult somatosensory cortex of rodents, the $\alpha 2$ enzyme almost completely co-localizes with the astrocytic glutamate transporters GLT-1 (SLC1A2) and GLAST (SLC1A3). Analysis at the ultrastructural level evidenced that this complex preferentially occurs in astrocytic processes around asymmetric glutamatergic synaptic junctions, but not around GABAergic terminals.¹⁶ The $\alpha 2$ isoform is thus assumed to be responsible for the buildup of Na^+ and K^+ gradients necessary for the glutamate uptake in this subcellular microdomain. Impaired $\alpha 2$ function should hence increase the susceptibility to SD based on the notion that SD is a reaction/diffusion mechanism in which neurons release neuroactive substances such as K^+ or glutamate. These are assumed to diffuse to adjacent neurons where they trigger a self-propagating regenerative process.^{67–70} Accordingly, impaired glutamate reuptake was reported in FHM2 knock-in mouse models.^{24,25}

An intriguing interpretation of our results is that the lack of one $\alpha 2$ allele is very well compensated under normal conditions and only becomes apparent in conditions of challenge. Prolonged exposure to elevated $[\text{K}^+]_o$ appears to be such a stressor. This interpretation is, in a broader sense, in agreement with data from a behavioral study of FHM2 knock-in mice ($\alpha 2^{+/G301R}$) that described stress-induced abnormalities when compared with WT.²⁴ Notably, however, elevated baseline $[\text{K}^+]_o$ represents a more extreme and in fact highly pathological stressor, which occurs for example during focal ischemia or after brain hemorrhage. Whereas hemolysis is the source of K^+ in brain hemorrhage,⁷¹ ischemia causes activation of Ca^{2+} -activated K^+ channels, resulting in a rise of baseline $[\text{K}^+]_o$, long before the ATP shortage slows the Na^+/K^+ -ATPases and SD occurs associated with further rapid rise of $[\text{K}^+]_o$.^{72,73}

Because expression of the $\alpha 2$ isoform is reduced by about $\sim 50\%$ in $\alpha 2^{+/KOE4}$ mice,²⁶ it is conceivable that the reduced gene dosage is unmasked only in conditions where transport capacity is exhausted and adaptation would require upregulation. Regulation of the intrinsic Na^+/K^+ -ATPase activity depends on substrate

concentration (K^+ , Na^+ , ATP), interaction with FXYP proteins and covalent modification, such as glutathionylation and phosphorylation.^{36,74} Further activity increase requires the insertion of additional Na^+/K^+ -ATPase enzymes into the plasma membrane through mobilization from endosomal pools,^{74,75} which might consequently unmask a reduced protein expression.

An additional mechanism could potentially aggravate $\alpha 2$ isoform deficiency under conditions of high $[K^+]_o$ load and promote decompensation of its homeostatic function: Previous studies have demonstrated a decrease of the ouabain-suppressible $\alpha 2/\alpha 3$ portion of the total Na^+/K^+ -ATPase activity in response to elevated baseline $[K^+]_o$. It has been suggested that this reduction did not result from loss of high-energy phosphate levels or modifications in protein or mRNA expression but from modifications of specific active sites, trapping the enzyme in an inactive phosphorylated state.⁷⁶

Pronounced post-SD oligemia in $\alpha 2$ -deficient mice

Mice deficient of the $\alpha 2$ isoform showed pronounced post-SD hypoemic responses. This could result from abnormal Ca^{2+} handling leading to enhanced vasoconstriction in the wake of SD. A multitude of studies have pointed to a distinct role of the $\alpha 2$ isoform in controlling local Ca^{2+} concentration and thereby modulating the release from intracellular Ca^{2+} stores.⁷⁷ Functional coupling of the $\alpha 2$ isoform with the Na^+/Ca^{2+} -exchanger (NCX)⁷⁸ was proposed as the mechanism by which the local Ca^{2+} concentration increases and in consequence the concentration in the endoplasmic/sarcoplasmic reticulum.⁷⁹ In the brain, the $\alpha 2$ isoform is highly expressed in glial and vascular smooth muscle cells (VSMCs) and the observed vasoconstrictive effect could be mediated by augmented intracellular Ca^{2+} transients in either cell type. In VSMCs and astrocytes, ouabain has been found to induce intracellular Ca^{2+} increases.^{12,15} Augmented Ca^{2+} transients in astrocytic endfeet were reported to cause constriction in arterioles.⁸⁰ The pronounced hypoemic rCBF response in $\alpha 2^{+/KOE4}$ mice is in agreement with data from $\alpha 2^{+/G301R}$ mice that have been described to exhibit enhanced contractility of cerebral arteries.⁸¹ This study identified higher Ca^{2+} sensitivity as opposed to increased Ca^{2+} release as the cause of enhanced contractility. The effect was reversible by cSrc inhibition. In addition, the resting blood flow in the middle cerebral artery was reduced in $\alpha 2^{+/G301R}$ mice.

Higher SD resistance of $\alpha 3$ -deficient mice in-vivo

Despite significant Na^+/K^+ -ATPase reduction in whole brain homogenates, $\alpha 3^{+/KOE4}$ mice were more resistant

against electrically induced SD in-vivo under urethane/ α -chloralose anesthesia compared to WT and displayed a lower SD speed. In a behavioral study, $\alpha 3^{+/KOE4}$ mice were shown to have a $\sim 40\%$ lower hippocampal NMDA receptor NR1 isoform expression compared to WT and more pronounced learning deficits compared to $\alpha 2$ -deficient mice.²⁶ One possible explanation of the decreased NMDA receptor expression is that chronic overexcitability during development may result in compensatory NMDA downregulation to reduce excitotoxic damage to neurons. Reduced glutamate receptor availability could explain the diminished efficiency of electrical SD induction since the induction process is likely to depend on glutamate release.⁸²

Conclusion

In summary, the data demonstrate distinct SD phenotypes as a consequence of genetic disruption or pharmacological inhibition of the three Na^+/K^+ -ATPase α isoforms expressed in the brain. Both, the astrocytic and neuronal isoform differentially affect the SD phenotype in heterozygous knock-out mice, whereas lack of one allele of $\alpha 1$, the ubiquitous isoform, had no significant effect on SD-associated features.

The dependence on additional external factors to reveal the SD phenotype in $\alpha 2^{+/KOE4}$ mice presents a mechanism that may model the episodic nature of migraine aura, where attacks depend on a combination of genetically determined susceptibility and challenging environmental conditions.⁸² In addition, the presented features of the different Na^+/K^+ -ATPase α isoforms are important for conditions during which the SD continuum is now increasingly recorded while the patient is on the neurocritical care unit, such as traumatic brain injury, intracerebral spontaneous hematoma, aneurysmal subarachnoid hemorrhage, malignant hemispheric stroke or cardiac arrest.^{1,83} Better understanding of the different isoforms could inform the development of novel therapeutic strategies in all these conditions.

Acknowledgements

We would like to thank Prof. Jerry B. Lingrel for generously providing heterozygous knock-out mice of ATP1A1, ATP1A2, and ATP1A3.

Author's contributions

Clemens Reiffurth: designed and performed experiments in-vivo, in acute brain slices and in-vitro, analyzed data, drafted and finalized the manuscript and approved the manuscript before submission. Mesbah Alam: designed and performed experiments in-vivo and in acute brain slices, analyzed data and approved the manuscript before submission. Mahdi Zahedi: designed and performed experiments in acute brain

slices, analyzed data and approved the manuscript before submission. Sebastian Major: designed experiments, analyzed data and approved the manuscript before submission. Jens Dreier: planned the study, designed experiments, analyzed data, drafted and finalized the manuscript and approved the manuscript before submission.


Funding

The author(s) disclosed receipt of the following financial support for the research, authorship, and/or publication of this article: This work was supported by Deutsche Forschungsgemeinschaft (DFG DR 323/5-1 and DFG DR 323/10-1), the Bundesministerium für Bildung und Forschung (Center for Stroke Research Berlin, 01 EO 0801) and FP7 no 602150 CENTER-TBI to Dr. Dreier.

Declaration of conflicting interests

The author(s) declared no potential conflicts of interest with respect to the research, authorship, and/or publication of this article.

ORCID iD

Jens P Dreier  <http://orcid.org/0000-0001-7459-2828>

Supplementary material

Supplementary material for this paper can be found at the journal website: <http://journals.sagepub.com/home/jcb>

References

- Dreier JP and Reiffurth C. The stroke-migraine depolarization continuum. *Neuron* 2015; 86: 902–922.
- Hartings JA, Shuttleworth CW, Kirov SA, et al. The continuum of spreading depolarizations in acute cortical lesion development: examining Leao's legacy. *J Cereb Blood Flow Metab* 2017; 37: 1571–1594.
- Engl E and Attwell D. Non-signalling energy use in the brain. *J Physiol* 2015; 593: 3417–3429.
- Astrup J, Sorensen PM and Sorensen HR. Oxygen and glucose consumption related to Na⁺-K⁺ transport in canine brain. *Stroke* 1981; 12: 726–730.
- Balestrino M, Young J and Aitken P. Block of (Na⁺,K⁺)ATPase with ouabain induces spreading depression-like depolarization in hippocampal slices. *Brain Res* 1999; 838: 37–44.
- Balestrino M. Pathophysiology of anoxic depolarization: new findings and a working hypothesis. *J Neurosci Methods* 1995; 59: 99–103.
- Kager H, Wadman WJ and Somjen GG. Conditions for the triggering of spreading depression studied with computer simulations. *J Neurophysiol* 2002; 88: 2700–2712.
- McGrail KM, Phillips JM and Sweadner KJ. Immunofluorescent localization of three Na,K-ATPase isozymes in the rat central nervous system: both neurons and glia can express more than one Na,K-ATPase. *J Neurosci* 1991; 11: 381–391.
- Orlowski J and Lingrel JB. Tissue-specific and developmental regulation of rat Na,K-ATPase catalytic alpha isoform and beta subunit mRNAs. *J Biol Chem* 1988; 263: 10436–10442.
- O'Brien WJ, Lingrel JB and Wallick ET. Ouabain binding kinetics of the rat alpha two and alpha three isoforms of the sodium-potassium adenosine triphosphate. *Arch Biochem Biophys* 1994; 310: 32–39.
- Moseley AE, Lieske SP, Wetzel RK, et al. The Na,K-ATPase alpha 2 isoform is expressed in neurons, and its absence disrupts neuronal activity in newborn mice. *J Biol Chem* 2003; 278: 5317–5324.
- Juhaszova M and Blaustein MP. Na⁺ pump low and high ouabain affinity alpha subunit isoforms are differently distributed in cells. *Proc Natl Acad Sci U S A* 1997; 94: 1800–1805.
- Hartford AK, Messer ML, Moseley AE, et al. Na,K-ATPase alpha 2 inhibition alters calcium responses in optic nerve astrocytes. *Glia* 2004; 45: 229–237.
- James PF, Grupp IL, Grupp G, et al. Identification of a specific role for the Na,K-ATPase alpha 2 isoform as a regulator of calcium in the heart. *Mol Cell* 1999; 3: 555–563.
- Song H, Lee MY, Kinsey SP, et al. An N-terminal sequence targets and tethers Na⁺ pump alpha2 subunits to specialized plasma membrane microdomains. *J Biol Chem* 2006; 281: 12929–12940.
- Similar perisynaptic glial localization for the Na⁺,K⁺-ATPase alpha 2 subunit and the glutamate transporters GLAST and GLT-1 in the rat somatosensory cortex. *Cereb Cortex* 2002; 12: 515–525.
- Rose EM, Koo JC, Antflick JE, et al. Glutamate transporter coupling to Na,K-ATPase. *J Neurosci* 2009; 29: 8143–8155.
- De Fusco M, Marconi R, Silvestri L, et al. Haploinsufficiency of ATP1A2 encoding the Na⁺/K⁺ pump alpha2 subunit associated with familial hemiplegic migraine type 2. *Nat Genet* 2003; 33: 192–196.
- de Carvalho Aguiar P, Sweadner KJ, Penniston JT, et al. Mutations in the Na⁺/K⁺-ATPase alpha3 gene ATP1A3 are associated with rapid-onset dystonia parkinsonism. *Neuron* 2004; 43: 169–175.
- Heinzen EL, Swoboda KJ, Hitomi Y, et al. De novo mutations in ATP1A3 cause alternating hemiplegia of childhood. *Nat Genet* 2012; 44: 1030–1034.
- Rosewich H, Thiele H, Ohlenbusch A, et al. Heterozygous de-novo mutations in ATP1A3 in patients with alternating hemiplegia of childhood: a whole-exome sequencing gene-identification study. *Lancet Neurol* 2012; 11: 764–773.
- Demos MK, van Karnebeek CD, Ross CJ, et al. A novel recurrent mutation in ATP1A3 causes CAPOS syndrome. *Orphanet J Rare Dis* 2014; 9: 15.
- Leo L, Gherardini L, Barone V, et al. Increased susceptibility to cortical spreading depression in the mouse model of familial hemiplegic migraine type 2. *PLoS Genet* 2011; 7: e1002129.
- Bottger P, Glerup S, Gesslein B, et al. Glutamate-system defects behind psychiatric manifestations in a familial hemiplegic migraine type 2 disease-mutation mouse model. *Sci Rep* 2016; 6: 22047.

25. Capuani C, Melone M, Tottene A, et al. Defective glutamate and K⁺ clearance by cortical astrocytes in familial hemiplegic migraine type 2. *EMBO Mol Med* 2016; 8: 967–986.
26. Moseley AE, Williams MT, Schaefer TL, et al. Deficiency in Na,K-ATPase alpha isoform genes alters spatial learning, motor activity, and anxiety in mice. *J Neurosci* 2007; 27: 616–626.
27. Eikermann-Haerter K, Dilekoz E, Kudo C, et al. Genetic and hormonal factors modulate spreading depression and transient hemiparesis in mouse models of familial hemiplegic migraine type 1. *J Clin Invest* 2009; 119: 99–109.
28. Brennan KC, Romero Reyes M, Lopez Valdes HE, et al. Reduced threshold for cortical spreading depression in female mice. *Ann Neurol* 2007; 61: 603–606.
29. Holmdahl R and Malissen B. The need for littermate controls. *Eur J Immunol* 2012; 42: 45–47.
30. Taylor CP, Weber ML, Gaughan CL, et al. Oxygen/glucose deprivation in hippocampal slices: altered intraneuronal elemental composition predicts structural and functional damage. *J Neurosci* 1999; 19: 619–629.
31. Kirov SA, Sorra KE and Harris KM. Slices have more synapses than perfusion-fixed hippocampus from both young and mature rats. *J Neurosci* 1999; 19: 2876–2886.
32. Schurr A, Reid KH, Tseng MT, et al. The stability of the hippocampal slice preparation: an electrophysiological and ultrastructural analysis. *Brain Res* 1984; 297: 357–362.
33. van den Maagdenberg AM, Pietrobon D, Pizzorusso T, et al. A Cacna1a knockin migraine mouse model with increased susceptibility to cortical spreading depression. *Neuron* 2004; 41: 701–710.
34. Oliphant TE. Python for Scientific Computing. *Computing in Science & Engineering* 2007; 9: 10–20.
35. Hunter JD. Matplotlib: a 2D graphics environment. *Comput Sci Eng* 2007; 9: 90–95.
36. Blanco G and Mercer RW. Isozymes of the Na-K-ATPase: heterogeneity in structure, diversity in function. *Am J Physiol* 1998; 275: F633–F650.
37. Heinemann U and Lux HD. Undershoots following stimulus-induced rises of extracellular potassium concentration in cerebral cortex of cat. *Brain Res* 1975; 93: 63–76.
38. Wallraff A, Kohling R, Heinemann U, et al. The impact of astrocytic gap junctional coupling on potassium buffering in the hippocampus. *J Neurosci* 2006; 26: 5438–5447.
39. Stoica A, Larsen BR, Assentoft M, et al. The alpha2beta2 isoform combination dominates the astrocytic Na(+)/K(+) -ATPase activity and is rendered nonfunctional by the alpha2.G301R familial hemiplegic migraine type 2-associated mutation. *Glia* 2017; 65: 1777–1793.
40. Tottene A, Conti R, Fabbro A, et al. Enhanced excitatory transmission at cortical synapses as the basis for facilitated spreading depression in Ca(v)2.1 knockin migraine mice. *Neuron* 2009; 61: 762–773.
41. Ayata C, Shin HK, Salomone S, et al. Pronounced hypoperfusion during spreading depression in mouse cortex. *J Cereb Blood Flow Metab* 2004; 24: 1172–1182.
42. Unekawa M, Ikeda K, Tomita Y, et al. Enhanced susceptibility to cortical spreading depression in two types of Na(+),K(+)-ATPase alpha2 subunit-deficient mice as a model of familial hemiplegic migraine 2. *Cephalalgia* 2018; 38: 1515–1524.
43. Ayata C and Lauritzen M. Spreading depression, spreading depolarizations, and the cerebral vasculature. *Physiol Rev* 2015; 95: 953–993.
44. Cain SM, Bohnet B, LeDue J, et al. In vivo imaging reveals that pregabalin inhibits cortical spreading depression and propagation to subcortical brain structures. *Proc Natl Acad Sci U S A* 2017; 114: 2401–2406.
45. Eikermann-Haerter K, Arbel-Ornath M, Yalcin N, et al. Abnormal synaptic Ca(2+) homeostasis and morphology in cortical neurons of familial hemiplegic migraine type 1 mutant mice. *Ann Neurol* 2015; 78: 193–210.
46. Dickinson R, Peterson BK, Banks P, et al. Competitive inhibition at the glycine site of the N-methyl-D-aspartate receptor by the anesthetics xenon and isoflurane: evidence from molecular modeling and electrophysiology. *Anesthesiology* 2007; 107: 756–767.
47. Saito R, Graf R, Hubel K, et al. Halothane, but not alpha-chloralose, blocks potassium-evoked cortical spreading depression in cats. *Brain Res* 1995; 699: 109–115.
48. Guedes RC and Barreto JM. Effect of anesthesia on the propagation of cortical spreading depression in rats. *Braz J Med Biol Res* 1992; 25: 393–397.
49. Kudo C, Nozari A, Moskowitz MA, et al. The impact of anesthetics and hyperoxia on cortical spreading depression. *Exp Neurol* 2008; 212: 201–206.
50. Takagaki M, Feuerstein D, Kumagai T, et al. Isoflurane suppresses cortical spreading depolarizations compared to propofol – implications for sedation of neurocritical care patients. *Exp Neurol* 2014; 252: 12–17.
51. Morth JP, Pedersen BP, Toustrup-Jensen MS, et al. Crystal structure of the sodium-potassium pump. *Nature* 2007; 450: 1043–1049.
52. Friedrich T, Tavraz NN and Junghans C. ATP1A2 mutations in migraine: seeing through the facets of an ion pump onto the neurobiology of disease. *Front Physiol* 2016; 7: 239.
53. Sykova E, Rothenberg S and Krekule I. Changes of extracellular potassium concentration during spontaneous activity in the mesencephalic reticular formation of the rat. *Brain Res* 1974; 79: 333–337.
54. Heinemann U and Lux HD. Ceiling of stimulus induced rises in extracellular potassium concentration in the cerebral cortex of cat. *Brain Res* 1977; 120: 231–249.
55. Prince DA, Lux HD and Neher E. Measurement of extracellular potassium activity in cat cortex. *Brain Res* 1973; 50: 489–495.
56. Futamachi KJ, Mutani R and Prince DA. Potassium activity in rabbit cortex. *Brain Res* 1974; 75: 5–25.
57. Vyskocil F, Kritz N and Bures J. Potassium-selective microelectrodes used for measuring the extracellular brain potassium during spreading depression and anoxic depolarization in rats. *Brain Res* 1972; 39: 255–259.

58. Karwoski CJ, Lu HK and Newman EA. Spatial buffering of light-evoked potassium increases by retinal Muller (glial) cells. *Science* 1989; 244: 578–580.
59. Walz W. Role of astrocytes in the clearance of excess extracellular potassium. *Neurochem Int* 2000; 36: 291–300.
60. Kofuji P and Newman EA. Potassium buffering in the central nervous system. *Neuroscience* 2004; 129: 1045–1056.
61. Walz W and Hertz L. Ouabain-sensitive and ouabain-resistant net uptake of potassium into astrocytes and neurons in primary cultures. *J Neurochem* 1982; 39: 70–77.
62. Grisar T, Franck G and Schoffeniels E. Glial control of neuronal excitability in mammals: II. Enzymatic evidence: two molecular forms of the (Na⁺),K⁽⁺⁾-ATPase in brain. *Neurochem Int* 1980; 2: 311–320.
63. Crambert G, Hasler U, Beggah AT, et al. Transport and pharmacological properties of nine different human Na, K-ATPase isozymes. *J Biol Chem* 2000; 275: 1976–1986.
64. Horisberger JD and Kharoubi-Hess S. Functional differences between alpha subunit isoforms of the rat Na,K-ATPase expressed in *Xenopus* oocytes. *J Physiol* 2002; 539: 669–680.
65. Kimelberg HK, Biddelcome S, Narumi S, et al. ATPase and carbonic anhydrase activities of bulk-isolated neuron, glia and synaptosome fractions from rat brain. *Brain Res* 1978; 141: 305–323.
66. Hajek I, Subbarao KV and Hertz L. Acute and chronic effects of potassium and noradrenaline on Na⁺, K⁺-ATPase activity in cultured mouse neurons and astrocytes. *Neurochem Int* 1996; 28: 335–342.
67. Dreier JP, Lemale CL, Kola V, et al. Spreading depolarization is not an epiphenomenon but the principal mechanism of the cytotoxic edema in various gray matter structures of the brain during stroke. *Neuropharmacology* 2018; 134: 189–207.
68. Zhou N, Rungta RL, Malik A, et al. Regenerative glutamate release by presynaptic NMDA receptors contributes to spreading depression. *J Cereb Blood Flow Metab* 2013; 33: 1582–1594.
69. Zandt BJ, ten Haken B and van Putten MJ. Diffusing substances during spreading depolarization: analytical expressions for propagation speed, triggering, and concentration time courses. *J Neurosci* 2013; 33: 5915–5923.
70. Moskowitz MA, Bolay H and Dalkara T. Deciphering migraine mechanisms: clues from familial hemiplegic migraine genotypes. *Ann Neurol* 2004; 55: 276–280.
71. Ohta O, Siguma M, Yamamoto M, Shimizu K and Toda N. *Cerebral vasospasm following ruptured intracranial aneurysms, especially some contributions of potassium ion released from subarachnoid hematoma to delayed cerebral vasospasm*. New York: Raven Press, 1998.
72. Erdemli G, Xu YZ and Krnjevic K. Potassium conductance causing hyperpolarization of CA1 hippocampal neurons during hypoxia. *J Neurophysiol* 1998; 80: 2378–2390.
73. Revah O, Lasser-Katz E, Fleidervish IA, et al. The earliest neuronal responses to hypoxia in the neocortical circuit are glutamate-dependent. *Neurobiol Dis* 2016; 95: 158–167.
74. Pirkmajer S and Chibalin AV. Na,K-ATPase regulation in skeletal muscle. *Am J Physiol Endocrinol Metab* 2016; 311: E1–E31.
75. Ewart HS and Klip A. Hormonal regulation of the Na⁽⁺⁾-K⁽⁺⁾-ATPase: mechanisms underlying rapid and sustained changes in pump activity. *Am J Physiol* 1995; 269: C295–311.
76. Mishra OP and Delivoria-Papadopoulos M. Cellular mechanisms of hypoxic injury in the developing brain. *Brain Res Bull* 1999; 48: 233–238.
77. Golovina VA, Song H, James PF, et al. Na⁺ pump alpha 2-subunit expression modulates Ca²⁺ signaling. *Am J Physiol Cell Physiol* 2003; 284: C475–486.
78. DiPolo R and Beauge L. Sodium/calcium exchanger: influence of metabolic regulation on ion carrier interactions. *Physiol Rev* 2006; 86: 155–203.
79. Moore ED, Etter EF, Philipson KD, et al. Coupling of the Na⁺/Ca²⁺ exchanger, Na⁺/K⁺ pump and sarcoplasmic reticulum in smooth muscle. *Nature* 1993; 365: 657–660.
80. Girouard H, Bonev AD, Hannah RM, et al. Astrocytic endfoot Ca²⁺ and BK channels determine both arteriolar dilation and constriction. *Proc Natl Acad Sci U S A* 2010; 107: 3811–3816.
81. Staehr C, Hangaard L, Bouzinova EV, et al. Smooth muscle Ca²⁺ sensitization causes hypercontractility of middle cerebral arteries in mice bearing the familial hemiplegic migraine type 2 associated mutation. *J Cereb Blood Flow Metab*. Epub ahead of print 7 March 2018. DOI: 10.1177/0271678X18761712.
82. Pietrobon D and Moskowitz MA. Pathophysiology of migraine. *Annu Rev Physiol* 2013; 75: 365–391.
83. Dreier JP, Major S, Foreman B, et al. Terminal spreading depolarization and electric silence in death of human cortex. *Ann Neurol* 2018; 83: 295–310.

9. Curriculum vitae

Mein Lebenslauf wird aus datenschutzrechtlichen Gründen in der elektronischen Version meiner Arbeit nicht veröffentlicht.

10. Complete list of publications

10.1 Articles

- 1) Dreier, J. P., S. Major, C. L. Lemale, V. Kola, **C. Reiffurth**, K. Schoknecht, N. Hecht, J. A. Hartings and J. Woitzik (2019). "Correlates of Spreading Depolarization, Spreading Depression, and Negative Ultraslow Potential in Epidural Versus Subdural Electrocorticography." *Frontiers in Neuroscience* 13(373). IF: 3.877
- 2) **Reiffurth, C.**, M. Alam, M. Zahedi-Khorasani, S. Major and J. P. Dreier (2019). "Na(+)/K(+)-ATPase α isoform deficiency results in distinct spreading depolarization phenotypes." *J Cereb Blood Flow Metab*: 271678X19833757. IF: 6.045
- 3) Eriksen, N., E. Rostrup, M. Fabricius, M. Scheel, S. Major, M. K. L. Winkler, G. Bohner, E. Santos, O. W. Sakowitz, V. Kola, **C. Reiffurth**, J. A. Hartings, P. Vajkoczy, J. Woitzik, P. Martus, M. Lauritzen, B. Pakkenberg and J. P. Dreier (2019). "Early focal brain injury after subarachnoid hemorrhage correlates with spreading depolarizations." *Neurology* 92(4): e326-e341. IF: 8.055
- 4) Dreier, J. P. and **C. Reiffurth** (2017). "Exploitation of the spreading depolarization-induced cytotoxic edema for high-resolution, 3D mapping of its heterogeneous propagation paths." *Proc Natl Acad Sci U S A* 114(9): 2112-2114. IF: 9.504
- 5) Dreier, J. P., M. Fabricius, C. Ayata, O. W. Sakowitz, C. William Shuttleworth, C. Dohmen, R. Graf, P. Vajkoczy, R. Helbok, M. Suzuki, A. J. Schiefecker, S. Major, M. K. Winkler, E. J. Kang, D. Milakara, A. I. Oliveira-Ferreira, **C. Reiffurth**, G. S. Revankar, K. ... B. MacVicar, T. Watanabe, J. Woitzik, M. Lauritzen, A. J. Strong and J. A. Hartings (2017). "Recording, analysis, and interpretation of spreading depolarizations in neurointensive care: Review and recommendations of the COSBID research group." *J Cereb Blood Flow Metab* 37(5): 1595-1625. IF: 6.045
- 6) Major, S., G. C. Petzold, **C. Reiffurth**, O. Windmuller, M. Foddiss, U. Lindauer, E. J. Kang and J. P. Dreier (2017). "A role of the sodium pump in spreading ischemia in rats." *J Cereb Blood Flow Metab* 37(5): 1687-1705. IF: 6.045

- 7) Dreier, J. P. and **C. Reiffurth** (2015). "The stroke-migraine depolarization continuum." *Neuron* 86(4): 902-922. IF: 14.318
- 8) Kondziella, D., C. K. Friberg, I. Wellwood, **C. Reiffurth**, M. Fabricius and J. P. Dreier (2015). "Continuous EEG monitoring in aneurysmal subarachnoid hemorrhage: a systematic review." *Neurocrit Care* 22(3): 450-461. IF: 3.163
- 9) Dreier, J. P., T. Isele, **C. Reiffurth**, N. Offenhauser, S. A. Kirov, M. A. Dahlem and O. Herreras (2013). "Is spreading depolarization characterized by an abrupt, massive release of gibbs free energy from the human brain cortex?" *Neuroscientist* 19(1): 25-42. IF: 7.461
- 10) Kang, E. J., S. Major, D. Jorks, **C. Reiffurth**, N. Offenhauser, A. Friedman and J. P. Dreier (2013). "Blood-brain barrier opening to large molecules does not imply blood-brain barrier opening to small ions." *Neurobiol Dis* 52: 204-218. IF: 5.227
- 11) Maslarova, A., M. Alam, **C. Reiffurth**, E. Lapilover, A. Gorji and J. P. Dreier (2011). "Chronically epileptic human and rat neocortex display a similar resistance against spreading depolarization in vitro." *Stroke* 42(10): 2917-2922. IF: 6.032
- 12) Tomkins, O., O. Friedman, S. Ivens, **C. Reiffurth**, S. Major, J. P. Dreier, U. Heinemann and A. Friedman (2007). "Blood-brain barrier disruption results in delayed functional and structural alterations in the rat neocortex." *Neurobiol Dis* 25(2): 367-377. IF: 5.227

10.2 Book chapters

- 1) Dreier, J. P., **C. Reiffurth**, J. Woitzik, J. A. Hartings, C. Drenckhahn, C. Windler, A. Friedman, B. MacVicar, O. Herreras and C. s. group (2015). *How spreading depolarization can be the pathophysiological correlate of both migraine aura and stroke*. In: Fandino J., Marbacher S., Fathi AR., Muroi C., Keller E. (eds) *Neurovascular Events After Subarachnoid Hemorrhage. Acta Neurochirurgica Supplement*, vol. 120. New York, NY: Springer New York; 2015. p. 137-140.
- 2) **Reiffurth C**, Kirov SA, Dreier JP. Spreading Depolarization. In: Chen J, Xu X-M, Xu ZC, Zhang JH, editors. *Animal Models of Acute Neurological Injuries II: Injury*

and Mechanistic Assessments, Volume 1. Totowa, NJ: Humana Press; 2012. p. 339-52.

- 3) Dreier JP, Winkler M, Wiesenthal D, Scheel M, **Reiffurth C**. Membrane Potential as Stroke Target. In: Lapchak PA, Zhang JH, editors. *Translational Stroke Research: From Target Selection to Clinical Trials. New York, NY: Springer New York; 2012. p. 295-303.*

11. Acknowledgements

Firstly, I would like to express my sincere gratitude to my advisor Prof. Dr. Jens Dreier for giving me the opportunity to work on this exciting topic, for his patience, his immense knowledge, his continued support and mentorship.

I am very grateful to my team colleagues that have made my work so much more enjoyable and who were available when I needed help. In particular, I would like to thank Dr. Sebastian Major, Dr. Ana Oliveira-Ferreira, Dr. Eun Jeung Kang, Dr. Nikolas Offenhauser, Stephan Haack, Dr. Karl Schoknecht, Dr. Maren Winkler, Dr. Denny Milakara and Coline Lemale. It was a great experience with all of you over the last years.

I would also like to thank my coworkers at the former Department of Neurophysiology at Tucholskystrasse in Berlin: Dr. Agustin Liotta, Dr. Christoph Behrens, Prof. Dr. Klaus Albus, Dr. Yaron David, Dr. Ezequiel Lapilover, Dr. Siegrun Gabriel and many more that have made my stay an unforgettable experience. With a special mention to Dr. Sebastian Ivens for his company, discussions and great parties. I would like to thank Dr. Gürsel Caliskan for enjoyable guitar jam sessions. Technical assistance, provided by Dr. Hans-Jürgen Gabriel and Bernhard Schacht, in particular with amplifiers for ion-selective microelectrodes, was greatly appreciated. I would like to express my very great appreciation to the late Prof. Dr. Uwe Heinemann who has always been open and welcoming and who has helped me immensely to improve my understanding of the fundamentals of neurophysiology.

From the University of Cincinnati, USA, I would like to thank Prof. Dr. Jerry Lingrel for generously providing heterozygous knock-out mice of ATP1A1, ATP1A2, and ATP1A3 and Dr. Amy Moseley for organizing the transport of the breeding pairs to the Charité – University Medicine campus.

I would like to thank Prof. Dr. Uli Dirnagl for his inspiration to rethink pre-clinical biomedical research and to focus on quality and reproducibility.

My special thanks are extended to the staff of the Experimental Neurology at the campus Mitte of the Charité – University Berlin who have greatly facilitated my lab work in vivo.

I also wish to acknowledge the help provided by Dr. Mahdi Zahedi-Khorasani whose excellent work in brain slices greatly contributed to this project.

My sincere thanks also go to the hard-working Dr. Mesbah Alam who will find a way to measure anything and for whom time does not exist. I am profoundly grateful for his generosity, great cooking and invaluable contribution to the project.

Last, but by no means least, I must express my very profound gratitude to my parents Marianne und Bernhard Reiffurth. Without their continued support my thesis would not have been possible.